

AN ABSTRACT OF THE THESIS OF

Zubaida A. Gulshan for the degree of Master of Science in
Nuclear Engineering presented on March 29, 1993.

Title: Fabric Composite Radiation Heat Transfer Study.

Redacted for privacy

Abstract Approved:

Andrew C. Klein

A Fabric Composite Radiation Heat Transfer Study has been conducted to determine the effective emissivities of specific fabric composite materials. The weave of the fabric and the high strength capability of the individual fiber in combination with the thermal conductivity and chemical stability of specific metallic liner, result in a very efficient light weight heat rejection system. Primary investigation included aluminum, copper, stainless steel and titanium as liner materials, and three different ceramic fabrics - Astroquartz II (a trademark of JPS Co., Slater, SC), Nextel (a trademark of 3M Co., St. Paul, MN) and Nicalon (a trademark of The Nippon Carbon Co., Japan). Experiments showed that fabric composite materials have significantly higher effective emissivities than the bare metallic liner materials. Aluminum and Astroquartz II combination and aluminum and Nextel combination appeared to be the most promising among the tested samples. To simulate deep space

the experiment was performed in vacuum where coolant fluid was circulated at about -10°C . The effective emissivity measurements were conducted at 376 K, 521 K and 573 K. Also high temperature effective emissivity measurements need to be performed.

Fabric Composite Radiation
Heat Transfer Study

by

Zubaida A. Gulshan

A THESIS

submitted to

Oregon State University

in partial fulfillment of
the requirements for the
degree of

Master of Science

Completed March 29, 1993
Commencement June 1993

APPROVED

Redacted for privacy

Associate Professor of Nuclear Engineering in charge of Major

Redacted for privacy

Head of Department of Nuclear Engineering

Redacted for privacy

Dean of Graduate School

Date thesis is presented _____ March 29, 1993.

Typed by Zubaida A. Gulshan

ACKNOWLEDGEMENTS

This work has been supported by the U.S. Department of Energy, Grant Number DE-FG07-89ER12901.

I wish to thank Dr. Andrew C. Klein for being a wonderful and friendly advisor and teacher. His subtle direction, continuous inspiration and unparalleled supervision at every step throughout this study deserves appreciation. I am sincerely thankful to him for giving me this opportunity to work with him.

Sincere thanks to H.H. Lee, W.C. Kiestler, S.A. Hamid, R. Snuggerud, T.S. Marks and Z. Huq who always helped me cheerfully.

I wish to thank professor M.S. Islam, Dr. S.I. Bhuiyan, and M. Musa for encouraging me to enter the field of nuclear engineering.

Finally I wish to thank the members of my family for consistently giving me moral support and appreciating all that I do. Special thanks to my parents. Special thanks to my husband for his endless efforts to make it all worthwhile.

Table of Contents

	<u>Page</u>
Chapter 1. Introduction and literature review	1
1.1. Introduction	1
1.2. Literature review	5
1.2.1. Compatibility test	6
1.2.2. Ceramic fabric wicking rate test	7
1.2.3. Fabric composite heat pipes	8
 Chapter 2. Theory of radiation heat transfer	 9
2.1. Theory	9
2.2.1. Analytical study	11
2.2.2. Boundary conditions	14
 Chapter 3. Design of the fabric composite radiation	
heat transfer test facility	15
3.1. Introduction	15
3.2. Fabrication procedure	15
3.2.1. Heating block	18
3.2.2. Cooling block	18
3.2.3. Thermal shields	19
3.2.4. Vacuum chamber	21
3.3.1. Heater	22
3.3.2. Advanced ceramic fabrics	23
3.4. Test procedure	24

Table of Contents Continued

	<u>Page</u>
Chapter 4. Results and discussions	31
4.1. Introduction	31
4.2. Results and analysis	31
4.2.1. Experimental results	31
4.2.2. Analytic results	36
4.2.3. Error analysis	39
4.3. Summary and conclusions	40
4.3.1. Disadvantages of the flat plate fabric composite heat transfer study experimental configuration	42
4.3.2. Recommendations for future work	44
Bibliography	45
Appendices	
Appendix A. Computer program hardcopies	48
Appendix B. Miscellaneous tables	71

List of Figures

<u>Figure</u>		<u>Page</u>
1.1.	Schematic of the rotating bubble membrane radiator	2
1.2.	Schematic of the SP100 space power system	3
1.3.	Schematic of the heat pipes in the heat radiator system of the SP100	3
2.1.	Schematic of the control volume approach of the combined conduction and radiation Heat Transfer Model for a Fabric Composite Structure	13
3.1.	Schematic of the fabric composite radiation heat transfer measurement experimental arrangement	16
3.2.	Schematic of the thermal shields	17
3.3.	Schematic of the flat plate electric heater screwed with the radiation shielding plates	17
4.1.	Comparison of effective emissivities of aluminum and fabric composite materials and bare aluminum liner material	32
4.2.	Comparison of effective emissivities of stainless steel and fabric composite materials and stainless steel liner	34
4.3.	Effective emissivities of various fabric composite materials at three different operating temperatures	35
4.4a.	Steady state temperature distribution in a copper liner at 376 K	38

List of Figures Continued

<u>Figure</u>		<u>Page</u>
4.4b.	Steady state temperature distribution in a copper liner at 521 K	38
4.4c.	Steady state temperature distribution in a copper liner at 573 K	39
4.5.	Effect of oxide coating on emissive properties of copper	43

List of Tables

<u>Table</u>	<u>Page</u>
Table I. Design parameters for the fabric composite radiation heat transfer experiment	30
Table II. List of ceramic fabric and metallic liner combinations chosen for primary investigation	30
Table III. List of fabric and liner combinations tested as initial investigation	31
Table IV. Parameters of the investigated ceramic fabrics	31
Table V. Dimensions of the investigated liner materials	31
Table VI. The uncertainty values in the measured parameters	41
Table VII. Summary of effective emissivity results and comparison	41

FABRIC COMPOSITE RADIATION HEAT TRANSFER STUDY

CHAPTER 1. INTRODUCTION & LITERATURE REVIEW

1.1. Introduction

For any space based nuclear power system, the waste heat ultimately has to be rejected to outer space. In a high temperature space power system the radiator of the heat rejection system must be constructed of materials having high emissivity in order to radiate heat efficiently. It is therefore very important to develop light weight, flexible heat rejection systems which can significantly enhance the heat radiation rate. The heat rejection system in space nuclear power reactors comprises a large portion of the total system mass and the exposed surface area. Therefore, a light weight fabric composite radiator would minimize the overall system mass by reducing the mass of this subcomponent. This reduction in mass will reduce the production and launch costs by a large amount.

Fabric composite radiators are one such light weight system and constructed of a low mass ceramic fabric panel for strength and micrometeorite protection, and a thin metallic sheet used to retain the working fluid. The combined advantages of lower mass, high structural strength and flexibility, and higher output capacity of the fabric

composite radiators makes the use of ceramic fabric composite materials as a potential candidate for space applications. Fabric composite materials will be used in fabric heat pipe radiators [1-3] and rotating bubble membrane radiators (RBMR) [4]. The RBMR is a space based heat rejection system which directly radiates waste heat to space [4]. The heat pipe is the most common traditional heat rejection system in the space nuclear power system. Figure 1.1 shows the schematic of the RBMR and Figure 1.2 and 1.3 include the schematic diagrams of the use of heat pipes in SP100 heat rejection system.

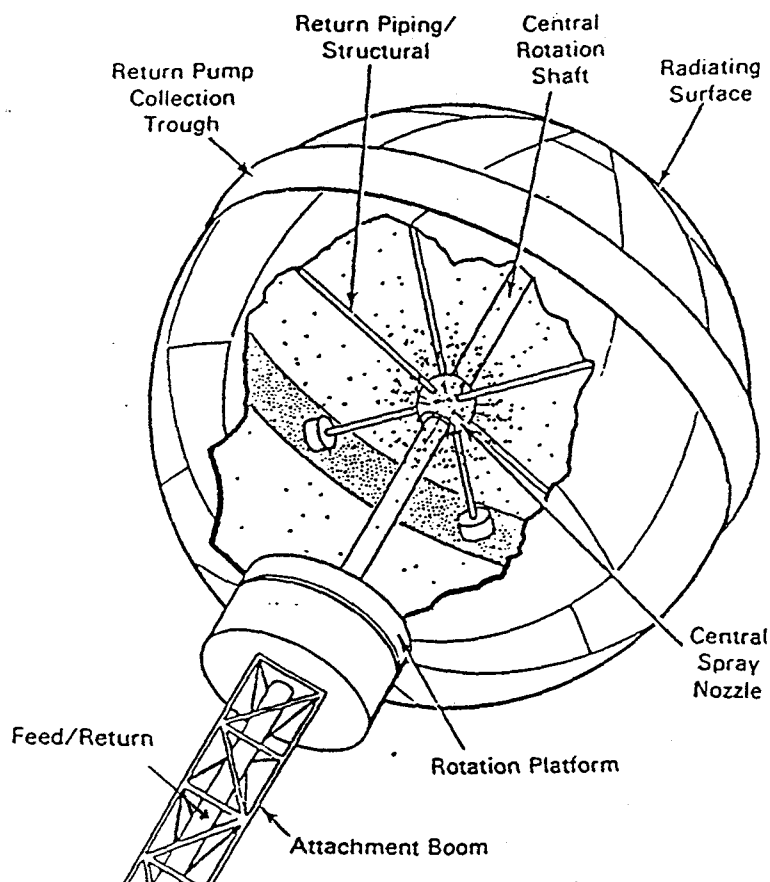


Figure 1.1. Schematic of the rotating bubble membrane radiator

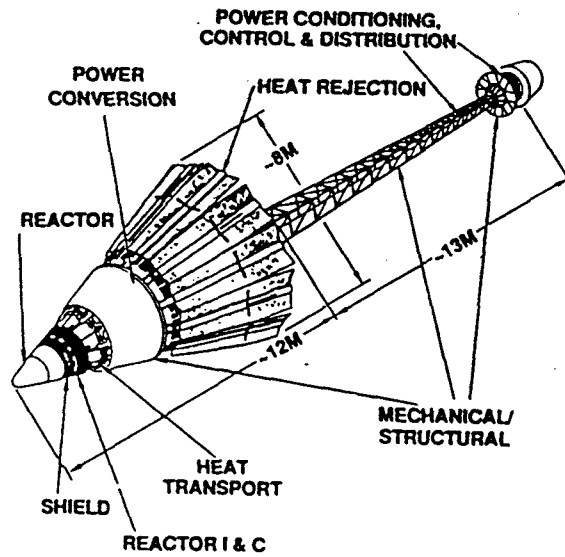


Figure 1.2 Schematic of the SP100 Space Power System

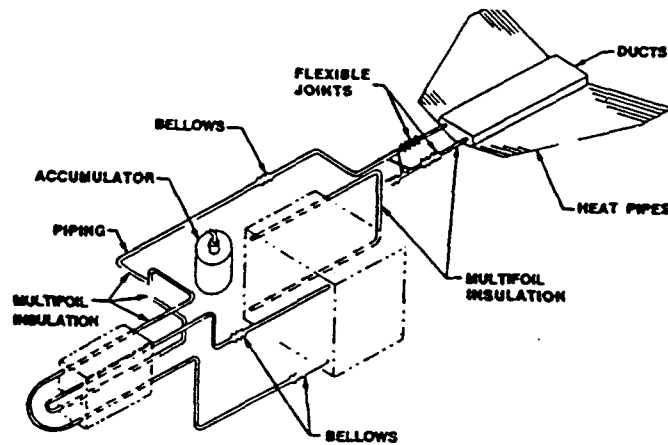


Figure 1.3 Schematic of the heat pipes in the heat radiator system of the SP100

The specific purpose of the fabric composite heat transfer study is to experimentally determine the effective emissivities of various fabric composite materials and to determine the best combination of fabric and liner material. The present study investigates the "effective" radiation heat transfer from a hot fabric-metal liner composite surface to a cooled surface to simulate the ultimate rejection of heat from a space based power system. The situation in this case is different than it is in a purely radiating environment. Here, in a combined conducting and radiating environment, covering a metallic surface with a ceramic fabric blanket would tend to increase the operating temperature of the metal surface. Such a fabric-metal liner composite can act to increase the radiating surface area due to the unevenness of the surface because of the multitude of strands of the woven material. This increase in surface area can greatly enhance the "effective emissivity" of the radiating surface, because effective emissivity of a radiating surface is directly related to the surface area. The "effective emissivity", as used in this context, is based upon the physical, or projected surface area of a radiating surface.

An investigation by M. S. El-Genk and H. Xue shows the effect of the radiator surface area of the decay heat rejection system for a lunar outpost [5]. It was found that the decay heat rejection period to reach a certain temperature

level, is decreased from 110 seconds to 20 seconds with an increase of the radiator surface area from 12.5 m^2 (134.55 ft^2) to 25 m^2 (269.09 ft^2).

The surface area of the radiating surface can be increased by roughening the surface also by other means such as, oxidation, weathering, sand blasting etc., which will also enhance the effective emissivity [6,7]. But the possible survivability of the advanced ceramic fabric composite material against the micrometeoroids, due to the structural strength, makes it more preferable.

1.2. Literature Review

In 1988 and 1989 Zenen I. Antoniak and Brent J. Webb indicated that fabric composite radiators will have superior performance characteristics with lower mass than most traditional radiators [8 & 9]. Nextel (a trademark of 3M Co., St. Paul, Minnesota, for alumina boria silica) was selected as the most promising fabric for space radiator applications because Nextel has excellent strength [9 & 10] and optical properties, and is readily available as a fiber (or filament) at a reasonable cost. Z. Antoniak et al performed preliminary tests with $.025 \text{ m}$ (.984 in) inner diameter Nextel tube which proved to have the required characteristics and yielded encouraging heat transfer data, when properly allied

with a metal or plastic liner [11]. Wicking tests were also done by Z. Antoniuk [11] which suggest that sufficient distributive wicking is supplied by the corrugations of the metal foil Advanced Ceramic Fabric (ACF) liner. More information about the ceramic fabrics is found in Chapter 3 and Appendix B2.

A significant amount of work has already been done on the fabric composite heat pipe radiator designs. Experiments have been conducted at Oregon State University to study different related properties of the ceramic fabrics [12-16]

1.2.1 Compatibility Test

Short term material compatibility with potential working fluids tests were conducted at Oregon State University from 1989 to 1990 and long term tests are being continued [12]. Specific materials tested include copper, aluminum, titanium and FEP teflon tubing and three high strength ceramic fabrics: Nicalon (a trademark of the Nippon Carbon Co., Japan), Nextel (a trademark of 3M Co., St. Paul, Minnesota) and Astroquartz (a trademark of JPS Co., Slater, South Carolina). Chemical compositions of Nicalon, Nextel and Astroquartz are silicon carbide, alumina boria silica and silicon dioxide respectively. These materials had been exposed to potential working fluids for up to 5000 hours at various temperatures

and have shown excellent compatibility with some of them [12]. It has been found that the best combinations of materials for the liner and working fluid for a fabric composite radiator would be aluminum and acetone, copper and acetone, titanium and water or FEP teflon with any of the three working fluids [14]. The combinations to be avoided include aluminum and water, copper and water and possibly methanol and copper and aluminum. It has also been found that the best combination of materials for the load bearing shell and working fluid would be silicon dioxide and either acetone or methanol, and possibly Nextel or Nicalon with either acetone or methanol. It was seen that the combination of Nextel with water must be avoided. Also both Nicalon and silicon dioxide did not seem to be as compatible with water.

1.2.2. Ceramic Fabric Wicking Rate Test

Several ceramic fabric materials have already been tested for determining the wicking velocity in a dry fabric at Oregon State University [13]. Presently studies are being conducted to obtain additional information on how well these materials will transport working fluids in heat pipes [15]. Results of these experiments show that the investigated ceramic fabric materials have very high wicking capacity, for example, a single layer of Nicalon wicks about 4,786 ml/hr-cm² of water at room temperature and pressure. Therefore it can

be concluded that the advanced ceramic fabric materials possess the key properties essential for space heat rejection system applications.

1.2.3. Fabric Composite Heat Pipes

The heat pipe is a heat transfer device readily adapted to space technology [17-20]. The light weight high strength fabric composite materials might be used as efficient heat rejection systems in the heat pipes. Experiments performed at Oregon State University and Battelle Pacific Northwest Lab, show great promise for the use of ceramic fabric composites for light weight heat pipes. A light weight fabric composite heat pipe (Stainless steel-Nextel combination) with a mass of .51 kg (1.124 lbs) rejects about 135 W/kg (208.94 Btu/hr-lb), where, a conventional heat pipe with a mass of 1.530 kg (3.37 lbs), rejects only 25 W/kg (38.69 Btu/hr-lb) [3].

Also, ultra light heat pipes, known as fabric composite reflux tubes were tested at Oregon State University and Battelle Pacific Northwest Lab. The heat rejection capacity of the reflux tube (using Copper-Nextel FC) is found to be about four times greater than that of light weight FC heat pipes, where the mass is reduced by about more than 3.5 times [3]. (mass 140 kg (.309 lb), rejected 500 W/kg (773.85 Btu/hr-lb)

CHAPTER 2. RADIATION HEAT TRANSFER

2.1. Theory

If a body is placed in the presence of cooler surroundings without any transport medium, it is observed to lose energy. This process is called thermal radiation. The thermal radiation emitted by a heated body is proportional to the fourth power of the body's temperature. Thus, for a given temperature difference, the heat transfer rate by thermal radiation is much greater at high temperature than at low temperature. The geometric configuration of bodies exchanging heat by this mechanism is also quite important. The thermal radiation emitted by one body that is intercepted by another is highly dependent on the size, shape and relative orientation of the bodies.

The basic law of thermal radiation is that the energy emitted by an ideal blackbody (a perfectly emitting body) is given by the Stefan-Boltzmann equation

$$q_r = A\sigma T^4 \quad 2.1$$

where, q_r is net the radiant heat energy, A is the body surface area, T is the absolute temperature of the body surface and σ is the Stefan-Boltzmann constant.

Not all radiating bodies behave as ideal blackbodies. A less than perfect emitting surface, called a gray surface,

emits according to

$$q_r = A\epsilon\sigma T^4 \quad 2.2$$

where, ϵ is known as the emissivity of the surface which is a physical property less than unity, and reflects the efficiency by which the surface will radiate thermal energy.

Equations 2.1 and 2.2 for black or gray bodies give only the emission of thermal radiation from those bodies. If a gray body with area A_s , body temperature T_s and surface emissivity ϵ_s , is completely surrounded by another surface which is very large when compared with the radiating surface, then the net radiant energy exchanged by the gray body and the surroundings is given by

$$q_r = A_s \epsilon_s \sigma_s (T_s^4 - T_e^4) \quad 2.3$$

where, T_e is the absolute temperature of the heat receiving surface. In equation 2.3 when q_r , A_s , σ_s , T_s and T_e are experimentally known, the emissivity can be calculated as follows -

$$\epsilon_s = \frac{q_r}{A_s \sigma_s (T_s^4 - T_e^4)} \quad 2.4$$

Equation 2.4 is used to calculate the effective emissivity in the flat plate fabric composite heat transfer study. It is obvious from equation 2.3 that the net radiant energy exchange is directly related to the surface area of the radiating surface. When the heated metallic surface is covered by a ceramic fabric in the fabric composite heat transfer study design configuration, the surface area is greatly increased, as has been discussed in Section 1.2.

2.2.1. Analytical Study

In order to model the fabric composite heat transfer experiment, a mathematical model based upon the combined conduction and radiation of heat through the fabric composite material and vacuum, is developed using numerical methods. A control volume cell approach is chosen to be a suitable tool for this modelling.

The presence of both integral and differential terms with different powers of temperature leads to a non-linear integro-differential equation. Moreover, in order to be able to calculate the radiation heat transfer through the fabric composite, the porosity of the fabric due to its weave pattern needs to be considered, and it will be necessary to consider the radiation heat transfer directly from the metallic liner through these pores into the vacuum. As the first step in the

modelling process, a simple conduction/radiation model is considered and the porosity of the fabric is neglected. To develop the basic governing equations for this modelling, the configuration shown in Figure 2.1 is considered [21]. Applying energy conservation laws to the one dimensional control volume in cell i gives,

$$(J_i - J_{i+1}) = -V_i S_i \quad 2.5$$

where, V_i is the volume of the cell i , and S_i is the volumetric heat source for cell i .

$$J_i = H_i A_i (T_{i-1} - T_i) \quad 2.6$$

$$J_{i+1} = H_{i+1} A_{i+1} (T_i - T_{i+1}) \quad 2.7$$

where, A_i and A_{i+1} are the areas of the cells, and H_i and H_{i+1} are the overall heat transfer coefficients defined as

$$H_i = \frac{2}{\frac{\Delta X_i}{K_i} + \frac{\Delta X_{i-1}}{K_{i-1}}} \quad 2.8$$

$$H_{i+1} = \frac{2}{\frac{\Delta X_i}{K_i} + \frac{\Delta X_{i+1}}{K_{i+1}}} \quad 2.9$$

where, K_i and K_{i+1} are the thermal conductivities of the cells. Then using the above definitions in equation 2.4 gives

$$H_i A_i (T_{i-1} - T_i) - H_{i+1} A_{i+1} (T_i - T_{i+1}) = -V_i S_i \quad 2.10$$

Substituting $C_i = H_i A_i$ and $C_{i+1} = H_{i+1} A_{i+1}$ equation 2.9 becomes

$$C_i T_{i-1} + C_{i+1} T_{i+1} - (C_i + C_{i+1}) T_i = -V_i S_i \quad 2.11$$

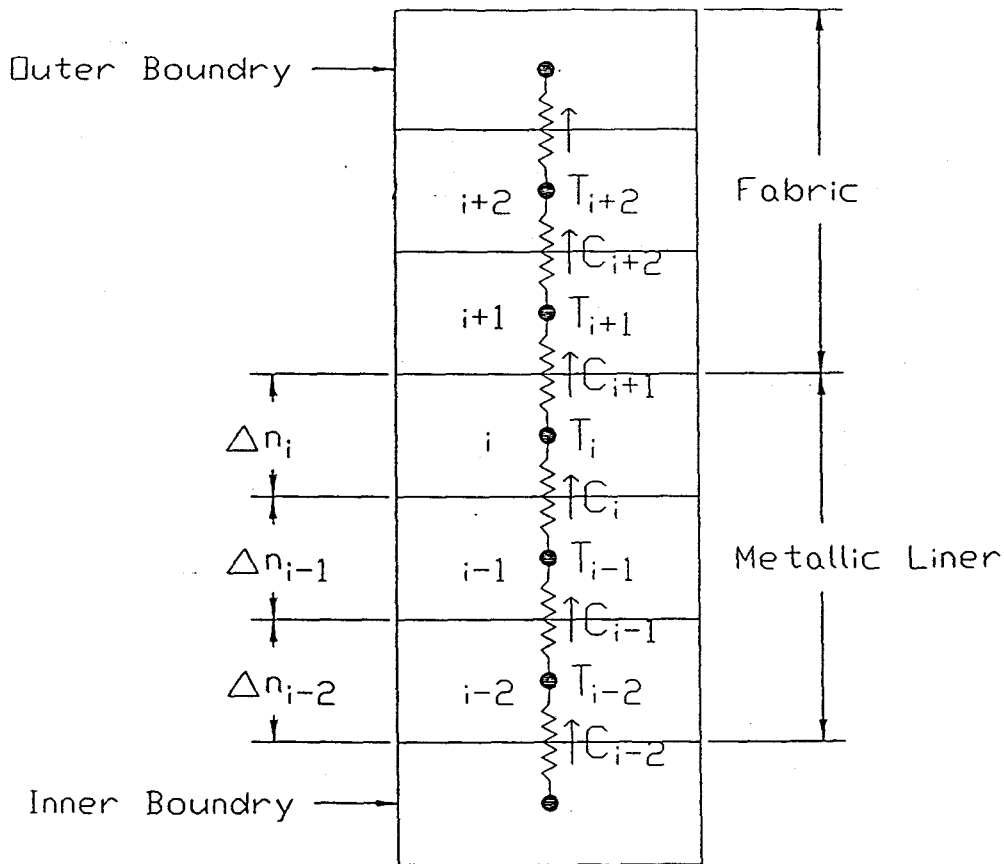


Figure 2.1. Schematic of the control volume approach of the combined conduction and radiation heat transfer model for a fabric composite structure

Hence it can be seen that the overall heat transfer coefficient H includes the material properties of the composite material. Equation 2.10 is therefore the governing equation for the model, and the heat flux at the inside boundary is incorporated into the source term S at the boundary. This equation is then solved for the temperature distribution within the fabric composite using the appropriate boundary conditions, i.e. the known heat flux on the inside surface and radiation heat transfer to the outside. A listing of the code developed for the analytical study has been included in the Appendix A1. Results of this study will be discussed in Chapter 4 to compare with experimental results.

2.2.2. Boundary Conditions

In any transport analysis two types of boundary conditions can occur:

- prescribed value of the variable on the boundary
- prescribed value of the gradient of the variable on the boundary.

In the one dimensional analytic heat transfer calculation, prescribed temperature boundary condition was applied on the hot and cold surfaces. On the two other sides, the second type of boundary condition was applied.

CHAPTER 3. DESIGN OF THE FABRIC COMPOSITE RADIATION HEAT TRANSFER TEST FACILITY

3.1. Introduction

The purpose of the Fabric Composite Radiation Heat Transfer experiment is to study the heat transfer from a hot fabric composite (FC) surface through a vacuum into a heat receiver to simulate the ultimate rejection of heat from a space based power system. The design objectives of the experimental facility are

- to determine the effective emissivities of various fabric composites materials
- to determine the effective emissivities of bare liner materials for comparison
- to determine the best combination of the fabric and liner material

3.2. Fabrication Procedure

The experimental apparatus has been constructed and a series of effective emissivity tests have been performed. In the final configuration, a vacuum vessel contains a uniform heating block at the top end and a uniform cooling block at the bottom end. The entire experimental arrangement is well insulated thermally from the environment using four stainless

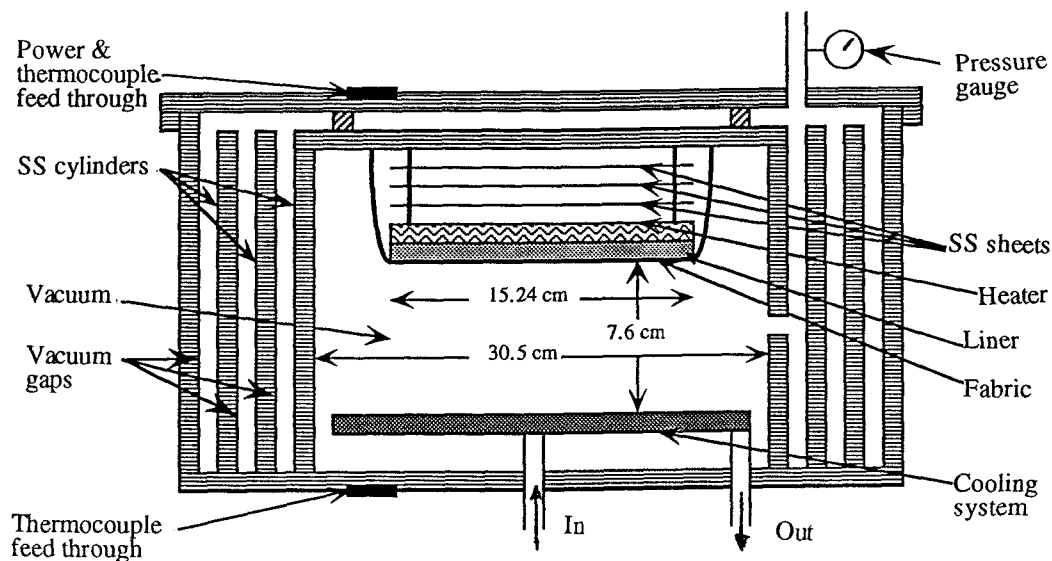


Figure 3.1. Schematic of the fabric composite radiation heat transfer measurement experimental arrangement

cylinders with small vacuum gaps in between to minimize undesired radiation heat loss from the inside. These small vacuum gaps act as thermal shields. Thus, it is expected that all of the heat passing through the fabric composite is radiated through the vacuum and ultimately received by the cooling system. The test facility is designed so that the heating block can be easily removed to change the fabric composite sample.

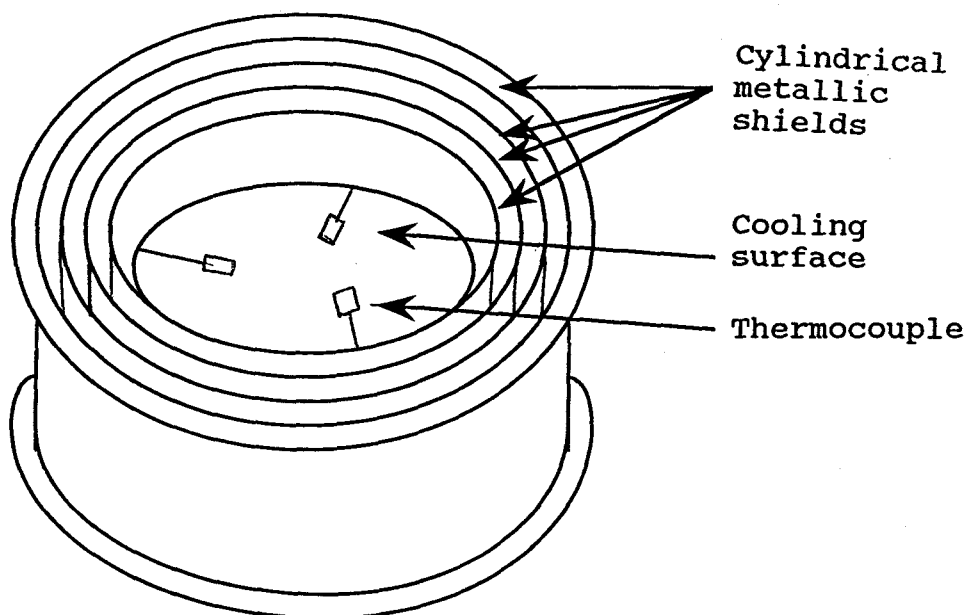


Figure 3.2. Schematic of the thermal shields

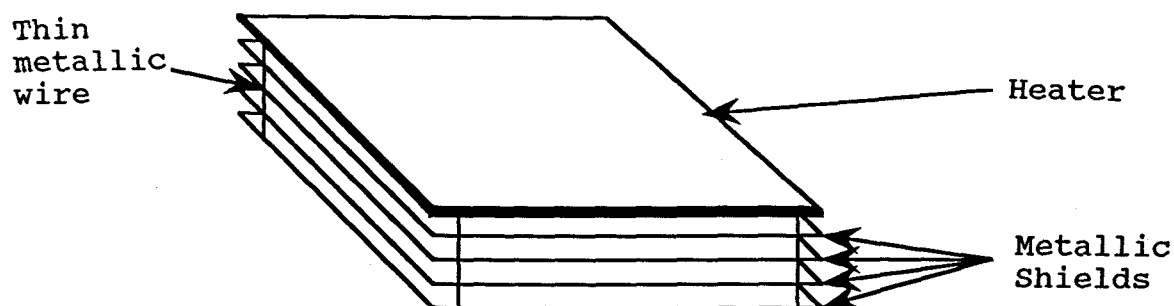


Figure 3.3. Schematic of the flat plate electric heater screwed with the radiation shielding plates

3.2.1. Heating Block

The fabric sample to be tested is placed on a flat electric heater and a metallic liner is sandwiched in between the heater and fabric as shown in Figure 3.1. This combination of the heater, liner and fabric is then inverted and hung from the lid of the vacuum vessel in an attempt to provide uniform contact between the heated surface and the FC. Detailed design procedure and dimensions are included in Figure 3.1.

The heater unit is thermally shielded on the back side by using four stainless steel plates connected by thin stainless steel wires with small vacuum spaces in between the plates. The combined weight of the stainless steel plates and the heater itself keeps the fabric composite stretched to maintain uniform contact with the heating surface. Three K-type thermocouples are attached to the heated surface to measure the radiating surface temperature (T_1). These thermocouples are thermally insulated by Nextel ceramic fabric tubing.

3.2.2. Cooling Block

A round disk shaped aluminum heat receiving system is placed opposite the heating block in the vacuum chamber. The heat receiving surface is 27.62 cm (10.875 inches) in

diameter and painted with a single layer of flat black paint to absorb heat efficiently. The cooling system is designed so that it can be pushed upward or downward to vary the distance between the heating and cooling blocks. A continuous flow of a 50% mixture of ethylene glycol and water is circulated from a chiller. Three K-type thermocouples are attached to the cooling surface to measure the cold surface temperature (T_2).

3.2.3. Thermal Shields

Appropriate thermal shields have been used to avoid any undesired heat loss from the inside of the Fabric Composite Heat Transfer facility. Four thin, smooth stainless steel (type 304) cylinders are placed inside the vacuum vessel surrounding the heating and cooling blocks with small (typically in the order of .5 - 1. cm) spaces in between, as shown in Figure 3.2. The same type of thermal shields are also used on the back side of the electric heater. Radiation heat exchange for the enclosure has been calculated by considering the side walls as well as the heat receiving surface as black bodies [6]. The equation used for this calculation is given below as

$$\sum_{j=1}^N \left(\frac{\delta_{kj} - F_{k-j}}{\epsilon_j} - F_{k-j} \frac{1 - \epsilon_j}{\epsilon_j} \right) \frac{Q_j}{A_j} = \sum_{j=1}^N (\delta_{kj} - F_{k-j}) \sigma T_j^4 \quad 3.1$$

where, N is the number of surfaces of the enclosure, Q/A 's are the heat fluxes across the corresponding surfaces, F 's are the view factors, T 's are the surface temperatures and δ_{kj} is the Kronecker delta defined as

$$\begin{aligned}\delta_{kj} &= 1 \quad \text{when } k = j \\ &= 0 \quad \text{when } k \neq j\end{aligned}$$

Corresponding to each surface, k takes on one of the values $1, 2, \dots, N$. When the surface temperatures are specified, the right hand side of equation 3.1 is known and there are N simultaneous equations for the unknown Q 's. The simultaneous equations are solved using a small matrix solver program which uses the tridiagonal method. In general, the heat inputs to some of the surfaces may be specified and the temperatures of these surfaces are to be determined. There are still a total of N unknown Q 's and T 's, and equation 3.1 provides the necessary number of relations. Since the values of emissivities depend on temperature, it is necessary initially to guess the unknown temperatures. Then the emissivity values can be chosen and the system of equations solved. The resulting temperature values can be used to select new emissivities, and the process repeated until the temperature and emissivity values no longer change upon further iteration. It can be noted that the results of this method will be approximate because the uniform radiosity assumption is not perfectly fulfilled over each finite area.

Calculations show that, using three metallic shields, the heat loss can be reduced to less than about two percent. Four shields have been used in the operation of the Radiation Heat Transfer facility as a conservative consideration, and it has been experimentally found that the heat transfer through the last shielding wall is less than two percent.

A small computer program developed to calculate the shape factors needed for the above calculations is included in Appendix A.

3.2.4. Vacuum chamber

The entire experimental system is contained within a 26.67 cm (10.5 inch) high stainless steel cylindrical pressure vessel with an inner diameter of 39.4 cm (15.5 inch). Heavy duty blind flanges have been welded to each end of the vessel, and the bottom endplate is permanently fixed to the vessel. The bottom has two small penetrations for the inlet to and outlet from the cooling system, and uses O-ring seals to provide a vacuum tight enclosure. The bottom also has a 6.35 cm (2.5 inch) hole into which the instrumentation feedthrough is fitted. This hole is covered by a teflon plate with an O-ring to keep the system vacuum tight. A three way valve is included with this endplate through which it is possible to draw a vacuum. The top endplate is removable, and has one

6.35 cm (2.5 inch) hole fitted with a teflon covering and O-ring. The teflon sheet is provided with one pair of leads for the electrical power connection, and five pairs of leads for thermocouples. The upper lid also has a pressure gauge to monitor the pressure inside the vessel. The upper end of the vessel uses a gasket and an O-ring to provide the vacuum seal. The volume of this pressure vessel is small enough and so that it is not required to meet the standards published in the ASME Boiler and Pressure Vessel Codes [22].

3.3.1. Heater

A high temperature electric heater has been designed with 15.24 cm (6 inch) on each side. This special heater is called an MI Strip heater and was purchased from the Watlow Heater Company, Portland, OR. The heater can be operated at up to 760°C (1400°F). It consists of a 10.69 mm (.042 inch) thick layer of mineral insulation which has nickel chrome element wire imbedded in it. This technology provides the heater with superb thermal conductivity, and yet retains a high dielectric strength. This thin layer of insulation results in the element wire being very close to the heater sheath. The top and bottom stainless steel sheath metals are welded together at the strategic points to maintain the high compaction of the insulation and produces a rigid, solid unit. Figure 3.3 shows the schematic diagram of the heater.

3.3.2. Advanced Ceramic Fabrics

Three types of advanced ceramic fabrics have been selected for this initial investigation - Nextel, Nicalon, and Astroquartz.

Nextel is a trademark of the 3M Co. and its chemical composition is Alumina Boria Silica. Nextel fabrics are woven from strong continuous Nextel fibers without the aid of organic, glass or metal inserts. It is a mullite composition of two percent added boria. It retains its strength and flexibility with little shrinkage at continuous temperatures of up to 1370°C (2500°F) [Appendix B2].

The Nicalon ceramic fabric is woven from continuous silicon carbide ceramic fiber manufactured through a polymer pyrolysis process by Nippon Carbon Co.. The fiber is homogeneously composed of ultrafine beta-SiC crystals with excess carbon and nine to eleven percent oxygen (as SiO₂). The fiber has excellent strength and modulus properties, and retains these properties at high temperatures [Appendix B2].

Astroquartz is a trademark of the JPS Co. and its chemical composition is silicon dioxide. Astroquartz II ceramic fabric is woven from Astroquartz II fiber yarns with 9779 resin compatible binder. The 9779 yarn binder is

compatible with many epoxy, bismaleimide, polyimide and phenolic resin systems. In addition to a proprietary aminosilane coupling agent, 9779 binder contains film formers and lubricants to facilitate weaving. It can be used at temperatures up to 1050°C [Appendix B2].

All three types of ceramic fabrics have been heat treated to remove their sizings prior to exposing them to high temperatures. Nextel is baked at 600°C for four hours, Nicalon and Astroquartz II are baked at 450°C for six hours to be cleaned. Typical physical and thermal properties of the investigated advanced ceramic fabrics are included in Appendix B.

3.4. Test Procedure

The experimental procedure followed for the effective emissivity measurement test is given below

1. The fabric is placed on the heater. The metal liner material is sandwiched in between the heater and the fabric.
2. The heating block is placed on the top lid of the vacuum vessel and electrically connected to the vessel lid by screws and bolts. The lid is then inverted so that the

heating block hangs loosely (see Figure 3.1).

3. The entire heating block assembly is then placed on top of the vacuum chamber, and the vacuum vessel is bolted closed.
4. A vacuum is drawn inside the pressure vessel. A moderate vacuum is sufficient for the experiment(about - 100 kilo Pascal). The pressure inside the apparatus is measured by a vacuum gauge.
5. The power switch, cooling, and rapid cooling switches to the chiller unit are turned on. Temperature and mass flow rate switches are set for the appropriate ranges. The coolant system valves are aligned.
6. Cooling liquid (at a temperature of about 263 K) is passed continuously through the cooling system from the chiller. The flow rate is monitored using a flow meter.
7. The heating block is heated up to the desired temperature. The temperature is controlled by adjusting the supplied voltage and current, and monitored using a multimeter.
8. After reaching thermal equilibrium at the desired

temperature (typically for 5 to 10 minutes), thermocouple readings are recorded to determine the temperature (T_1) of the radiating surface (heater surface). The cooling system surface temperature (T_2) is also recorded at the same time using thermocouples to determine the heat received. An electronic data logger is used to record the readings.

9. Knowing the current and voltage supplied from the power supply unit, the effective emissivity of the fabric composite is calculated using equation 3.2.
10. The power supply unit is adjusted to a higher voltage to heat the heater unit to the desired higher temperature and steps 6 to 9 are repeated.
11. At the end of the tests, the power supply unit is turned off and all of the meters are unplugged. The chiller unit is turned off and the three way valve is opened slowly to release the vacuum.

The heating surface temperature (T_1) and cooling surface temperature (T_2) are noted from the data logger. The effective emissivity of the fabric composite material is calculated using the radiation heat transfer equation mentioned in Section 2.1 (equation 2.3), which is repeated

below as

$$Q/A = \epsilon \sigma (T_1^4 - T_2^4) \quad 3.2$$

where,

- T_1 = liner surface temperature (K)
- T_2 = cold surface temperature (K)
- Q = amount of heat transferred (watts)
- A = area of the heated surface (cm²)
- σ = Stefan-Boltzmann constant (W/cm²-s-K⁴)
- ϵ = effective emissivity of the fabric composite based on the heater surface temperature

A small FORTRAN program has been developed and used to calculate the effective emissivity using equation 3.2. The program listing is included in Appendix A. The program uses voltage, current, heating surface temperature, and heat receiving surface temperature as input, and prints the desired effective emissivity as output.

Also, thermocouples are placed on the outside walls of the cylinders to measure any undesired heat loss through the walls. Knowing the temperatures on the outside wall of the last shield (when going outward) and the inside wall of the vacuum chamber, the heat transfer across the chamber wall, is calculated using equation 3.2. Typically the heat loss is found to be less than two percent.

The design parameters for the experiment are listed in Table I. A complete list of composite materials combinations of interest which could be investigated include - copper and alloys, titanium and alloys, aluminum and alloys, stainless steel, molybdenum and teflon as working fluid retention liner materials and three different ceramic fabrics - Nicalon, Nextel and Astroquartz with all weave patterns. Kevlar is also a type of strong ceramic fabric made from continuous aramid fiber, but it can not be used above 200°C. Compatibilities of these liner and fabric materials with the possible working fluids have been discussed in Section 1.3.1. Useful parameters that can be adjusted for the experiment include the fabric composition, weave pattern, weave density, liner composition and surface temperature. The fabric-metal combinations which have been tested as the initial investigation are given in Table III. Other useful parameters of the investigated fabric and liner materials are listed in Tables IV and V respectively.

Table I. Design parameters for the fabric composite radiation heat transfer experiment.

Maximum temperature	800 K
Maximum power input	500 Watts
Heat flux	$\approx 3 \text{ Watts/cm}^2$
Mass flow rate of the coolant	$\approx 2 \text{ kg/min}$
Cooling liquid	A mixture of ethylene glycol (50%) and water(50%)

Table II. List of ceramic fabric and metallic liner combinations chosen for primary investigation.

Fabric & liner	Fabric & liner	Fabric & liner
Astroquartz & aluminum	Nextel & aluminum	Nicalon & aluminum
Astroquartz & stainless steel	Nextel and stainless steel	Nicalon & stainless steel
Astroquartz & copper	-	Nicalon copper
Astroquartz & titanium	Nextel & titanium	Nicalon & titanium
Astroquartz & molybdenum	Nextel & molybdenum	Nicalon & molybdenum
Astroquartz & teflon	Nextel & teflon	Nicalon & teflon

Table III. List of fabric and liner combinations tested as initial investigation.

Fabric & liner	Fabric & liner	Fabric & liner
Astroquartz II & aluminum	Nicalon & aluminum	Nextel & aluminum
Astroquartz II & stainless steel	Nicalon & stainless steel	Nextel & stainless steel
Astroquartz II & copper	Nicalon & copper	
Astroquartz II & titanium		

Table IV. Parameters of the investigated ceramic fabrics.

Fabric	Weave pattern	Weight (g/m ²)	Chemical composition
Nextel	5H satin	474.0	Alumina boria silica
Nicalon	plain	280.0	Silicon carbide
Astroquartz II	8H satin	284.61	Silicon dioxide

Table V. Dimensions of the investigated liner materials

Material	Length (cm)	Width (cm)	Thickness (mm)
Aluminum	15.24	15.24	2.0
Stainless steel	15.24	15.24	2.0
Copper	15.24	15.24	3.0
Titanium	15.24	15.24	2.0

CHAPTER 4. RESULTS AND DISCUSSIONS

4.1. Introduction

The primary objective of the fabric composite heat transfer study is to evaluate the effective emissivities of different fabric composite materials and to determine the best combination, also, to compare with that of the uncovered liner material. Results of the primary investigation of the fabric composite materials listed in Table III, are discussed in the following section.

4.2. Results and Analysis

4.2.1. Experimental Results

The initial investigation has been performed using the following fabric composites - Nextel and aluminum, Nextel and stainless steel, Nicalon and aluminum, Nicalon and stainless steel, Nicalon and copper, Astroquartz II and aluminum, Astroquartz II and stainless steel, Astroquartz II and copper, Astroquartz II and titanium, at three different operating temperatures. A conservative estimate based on experimental measurements of ten percent radiation heat loss from the system has been considered for the calculations. Measurements of the thermal shield temperatures show that less

than two percent of the heat is lost through the side walls and less than two percent is lost through the top lid of the vacuum vessel. Therefore five percent heat loss has been estimated each way as conservative consideration.

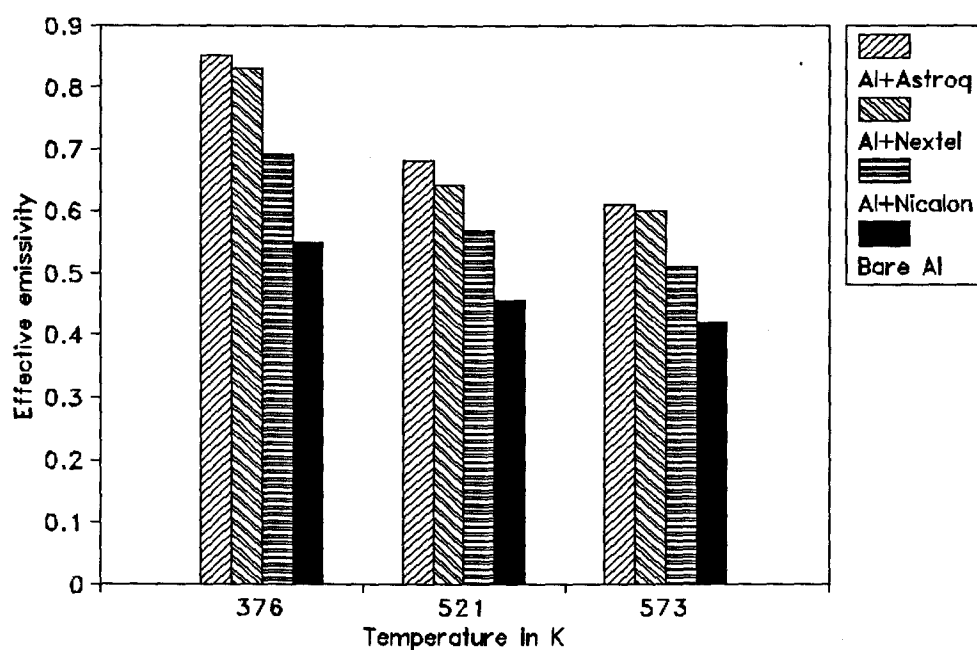


Figure 4.1. Comparison of effective emissivities of aluminum and fabric composite materials and bare aluminum liner material.

Figure 4.1 shows the graphical representation of the effective emissivities for a bare aluminum liner and for three different ceramic fabrics in combination with the aluminum liner. It can be seen from Figure 4.1 that the Astroquartz II and aluminum combination has about seventy five percent greater effective emissivity than the bare aluminum liner at 103°C (217.4°F). In general, any of the fabric composite combinations in Figure 4.1 show significantly higher effective emissivity than the bare aluminum liner at the three operating temperatures. Figure 4.2 shows the same trend for a stainless steel liner. Again, the effective emissivities of the fabric composites are significantly higher than the effective emissivity of the bare stainless steel liner. The possible reason for this enhancement in the effective emissivities, is the large increase in the effective radiating surface area of the fabric over that of a bare metal surface since emissivity is a radiating surface property of a material. As has been discussed in Chapter 1, this increase in the radiating surface area is due to the woven nature of the fabric.

The effective emissivity obtained for the Nextel and stainless steel combination using the cylindrical geometry of the fabric composite heat pipe test facility is $0.69 \pm .04$ at 160°C (320°F) [3]. This value is comparable with the flat plate configuration result tested at 103°C (217.4°F). The values reported in reference 1 for the same combination is

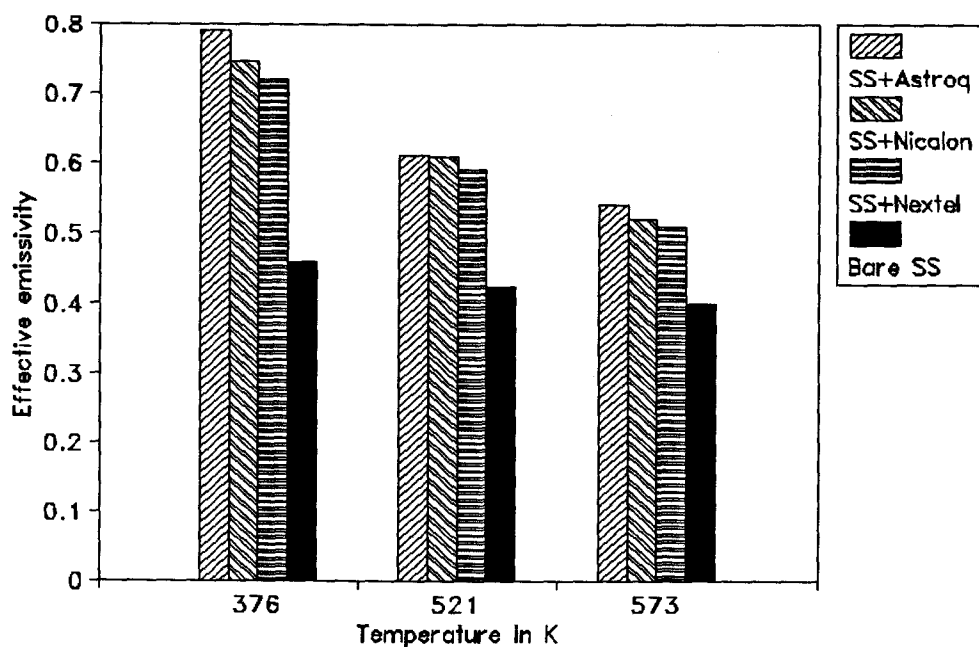


Figure 4.2. Comparison of effective emissivities of stainless steel and fabric composite materials and stainless steel liner material.

much lower than the flat plate configuration results. This discrepancy may be is because of the difference in the choice of the weave pattern or fabric density, or experimental arrangement. Another reason may be the much higher radiating surface temperature (447 °C-527 °C) used by Antoniak et al[1].

It can be stated at this point that, there is no possibility of convective heat transfer in this experimental

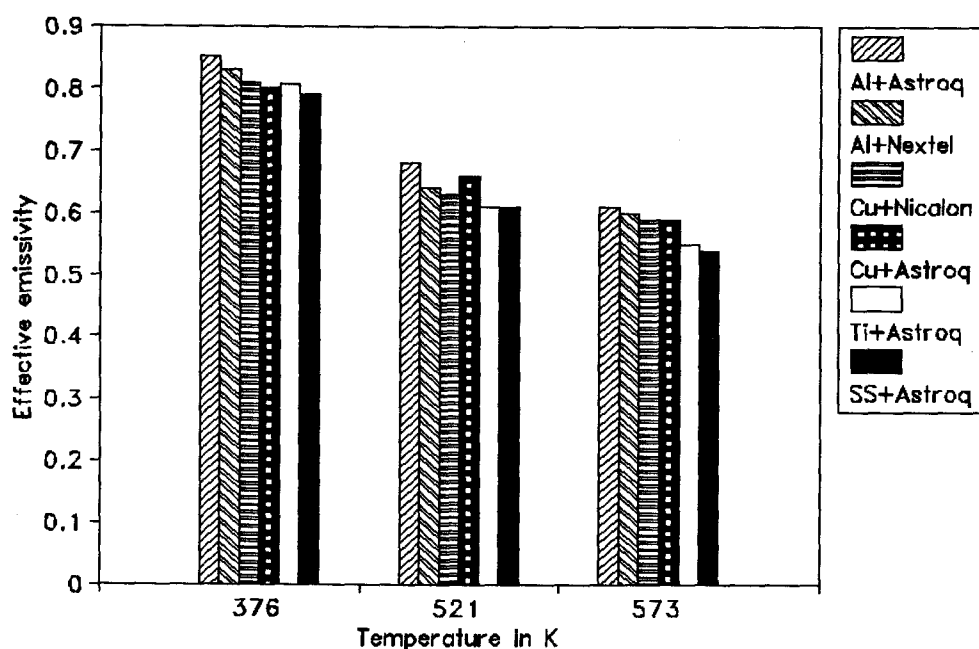


Figure 4.3. Effective emissivities of various fabric composite materials at three different operating temperatures.

arrangement because of the orientation of the heated block on the top and the cold block on the bottom of the vacuum chamber which has a negative pressure of about 100 kilo Pascal. According to the kinetic theory of gases at raised temperatures [23] the slightest possible remaining gas becomes stratified, which may lead to some conductive heat transfer. To estimate the conductive heat transfer, the thermal conductivity of air at the reduced pressure and relative temperature was calculated using the thermal conductivity at the critical temperature and pressure [23]. The heat

transferred by conduction was calculated using this thermal conductivity, and it was found, that conduction contributes less than one percent to the total heat transfer in the system. Also, it was experimentally found that, at atmospheric pressure and at sufficiently elevated temperature, the heat transferred through the stratified air in the chamber by conduction is considerably lower than the heat transferred by radiation. To evaluate this, a test was performed using an Astroquartz II and aluminum composite and no vacuum was drawn. Therefore, all of the heat was considered to be conducted through air at atmospheric pressure. The heat transferred by conduction in this case was found to be $0.48\text{E-}02$ watts/cm² at 103 °C, compared to about $8.0\text{E-}02$ watts/cm² by the radiative heat transfer process, using the same fabric composite material at the same operating temperature. Therefore it can be stated that, even if there was any chance of leakage in the vacuum, the contribution of conductive heat transfer process is negligible.

4.2.2. Analytic Results

It is found that the results obtained experimentally match very well with the analytical results. As was mentioned earlier in Chapter 2, a computer program has been developed to calculate the heat transfer using numerical methods, for comparison. With specified boundary conditions, the program

calculates the temperature distribution, and also, the heat flux for a given effective emissivity, or, vice versa. As an example, the heat flux passing through the bare copper liner from the heated surface is found to be $4.4\text{E-}02 \text{ W/cm}^2$ at 103°C (217.4°F), $18.55\text{E-}02 \text{ W/cm}^2$ at 248°C (478.4°F), and $24.79\text{E-}02 \text{ W/cm}^2$ at 300°C (572°F). The experimentally determined effective emissivities have been used in computing these values. The results match reasonably well with the experimental results which are $4.33\text{E-}02 \text{ W/cm}^2$, $18.54\text{E-}02 \text{ W/cm}^2$ and $24.77\text{E-}02 \text{ W/cm}^2$ respectively for the corresponding radiating surface temperatures and effective emissivities. The deviation is less than \pm two percent. Similarly, for the bare aluminum liner, the results differ by about \pm one percent at 521 K and 573 K and about four percent at 376 K. The calculated values are $5.74\text{E-}02 \text{ W/cm}^2$, $20.04\text{E-}02 \text{ W/cm}^2$ and $27.72\text{E-}02 \text{ W/cm}^2$ at 376°C , 521°C and 573°C respectively. The corresponding experimental values are found to be $5.43\text{E-}02 \text{ W/cm}^2$, $20.11\text{E-}02 \text{ W/cm}^2$ and $27.82\text{E-}02 \text{ W/cm}^2$ respectively. Better agreement with the experimental results could be achieved using finer mesh grid system. Figures 4.4a, 4.4b and 4.4c include the steady state temperature distributions in the copper liner sheet at the three different operating temperatures, obtained using the computer program FCRHT [Appendix A1].

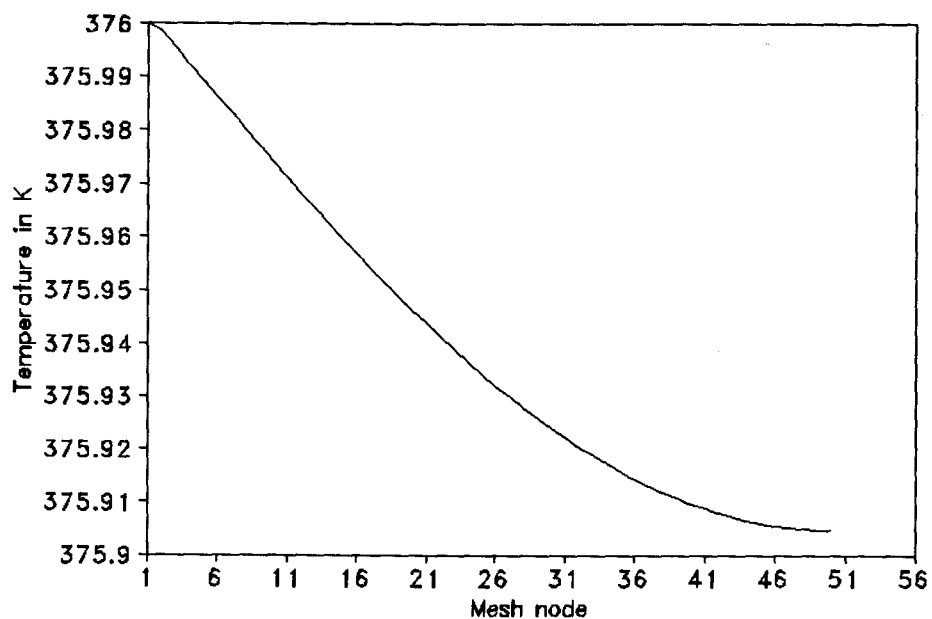


Figure 4.4a. Steady state temperature distribution in a copper liner at 376 K.

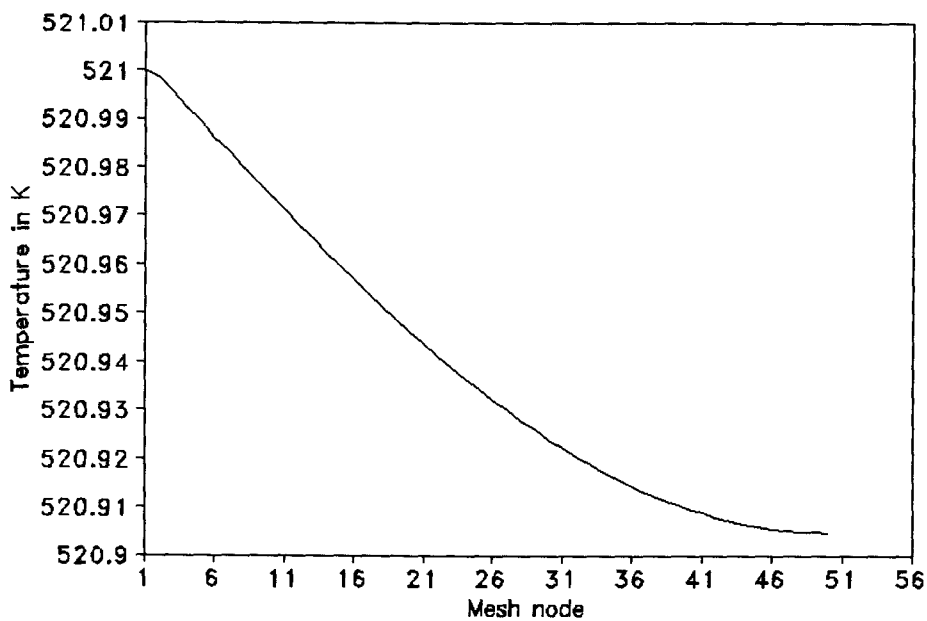


Figure 4.4b. Steady state temperature distribution in a copper liner at 521 K.

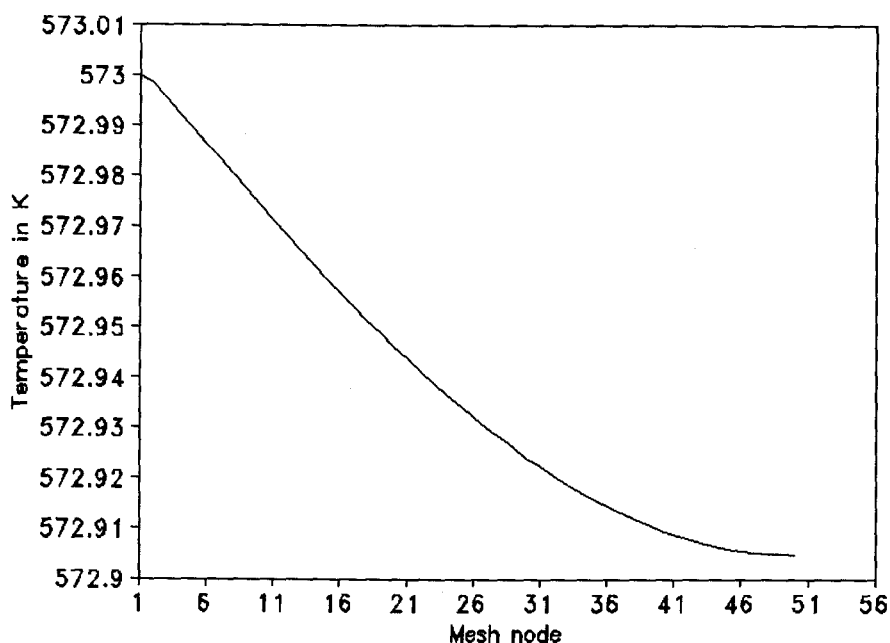


Figure 4.4c. Steady state temperature distribution in a copper liner at 573 K.

4.2.3. Error Analysis

In the process of radiation heat transfer calculation, the uncertainty values which might affect the effective emissivity most are those in the measured parameters. These uncertainties arise due to the accuracy and tolerance of the instrumentation. The uncertainty parameters considered for the values measured in the effective emissivity test are listed in Table VI. To take care of the uncertainty in Q_{in} , 10 percent reduction in power due to heat loss from the system as a whole was estimated based upon experimental measurements. This has been discussed in Section 4.2.1. The uncertainties

in the temperature measurements were obtained from the standard deviations of a large number of readings taken. The uncertainties were assumed to be random and independent. Total uncertainty was calculated using the error propagation formula [24] given below,

$$\sigma^2\epsilon = \left(\frac{\delta\epsilon}{\delta T_1}\right)^2\sigma^2T_1 + \left(\frac{\delta\epsilon}{\delta T_2}\right)^2\sigma^2T_2 + \dots \quad 4.1$$

where $\epsilon = \epsilon(T_1, T_2, \dots)$ represents the derived quantity. The total uncertainties in the effective emissivities have been included in Table VII. A routine to calculate the uncertainties associated with the experiments is included in the emissivity calculation program listed in Appendix B.

4.3. Summary and Conclusions

It can be concluded from the experimental results that, the Advanced Ceramic Fabric Composite Materials furnish significantly higher values of effective emissivities than the bare metallic liner materials. From the results obtained so far, the Astroquartz II and aluminum combination appeared to be the best fabric composite material. The results plotted in Figures 4.1 - 4.3 (also listed in Table VII) indicate that the investigated fabric composite materials have very close effective emissivities and any of the combinations is recommendable for desired space application.

Table VI. The uncertainty values in the measured parameters.

Parameters	Uncertainty Values
Q_{in}	10 % of the overall
T_1	2 °C
T_2	2 °C

Table VII. Summary of effective emissivity results and comparison

FC	Temperature 376 K		Temperature 521 K		Temperature 573 K	
	ϵ	Q/A (W/m ²)	ϵ	Q/A (W/m ²)	ϵ	Q/A (W/m ²)
Al+Astroq.	.85 ±.004	820	.68 ±.004	2954	.61 ±.003	3946
Al+Nextel	.83 ±.004	816	.63 ±.003	2727	.6 ±.003	3931
Cu+Nicalon	.81 ±.004	780	.64 ±.003	2820	.59 ±.003	3916
Cu+Astroq.	.8 ±.004	785	.66 ±.003	2834	.59 ±.003	3893
Ti+Astroq.	.81 ±.004	794	.61 ±.003	2677	.55 ±.003	3615
SS+Astroq.	.79 ±.004	779	.61 ±.003	2689	.54 ±.003	3536
SS+Nicalon	.75 ±.004	733	.6 ±.003	2653	.52 ±.003	3348
SS+Nextel	.72 ±.004	720	.59 ±.003	2591	.51 ±.003	3339
Al+Nicalon	.69 ±.004	688	.56 ±.003	2492	.51 ±.003	3353

4.3.1. Disadvantages of the Flat Plate Fabric Composite Heat Transfer Study Experimental Configuration

The effective emissivities of the fabric composites are directly related to how well the contact between the liner and the fabric, is maintained. The contact resistance between the fabric and the liner is high in the flat plate radiation heat transfer design and it is very low in the heat pipe design because of the cylindrical shape of the heat pipe. At raised temperatures the stainless steel pipe expands and the cylindrical shape provides a uniform and tight contact to the ceramic fabric shell.

The bare metal effective emissivities recorded for both aluminum and stainless steel, appeared to be slightly higher than the text book values reported for them (see Appendix B1). One possible reason for this may be the distortions caused by the metallic clips used for attaching the bare liner to the hot surface.

Also, it is evident from the results that the effective emissivities of the Fabric Composites have a trend of decreasing with the increasing temperature. Possibly, this is the effect of surface roughness caused by covering the metal liner by the ceramic fabric. The emissivity of a dielectric surface decreases with increasing temperature [6]. The same

trend is noticed when a metallic surface is roughened by some other means such as, oxidation, sand blast, weathering etc. (see Figure 4.5). Another possible reason for the decrease of the effective emissivities is that, with the increase of the temperature, the physical properties of the ceramic fabrics are changed (although negligibly).

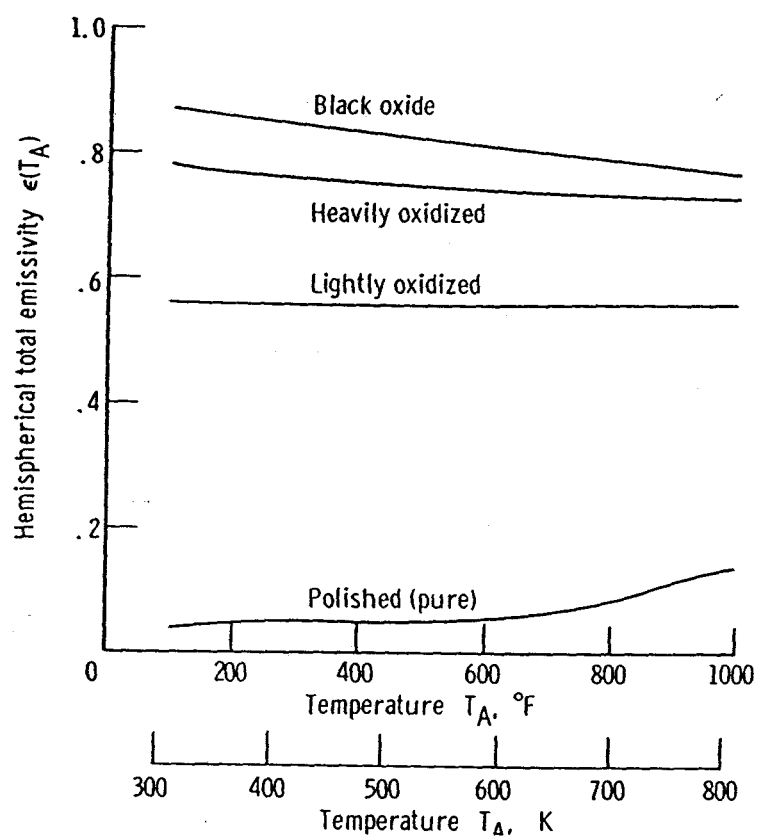


Figure 4.5. Effect of oxide coating on emissive properties of copper

4.3.2. Recommendations for Future Work

To achieve uniform and tight contact between the fabric and the liner material, it is needed to revise the current experimental facility. It seems to be reasonable that a cylindrical shape for the heated surface, like it is in the heat pipe design, will provide the desired level of uniform proximity with the radiating fabric surface. Therefore, in the future, the heating block needs to be redesigned with slightly convex heated surface. Also it can be suggested that, the electric heater be manufactured with an **on/off** switch. Additionally, it will be very useful to conduct the investigations on various additional fabric types, weave patterns and densities as well as at more elevated operating temperatures.

Another area to be worked on, is the computer modelling, considering the representation of the ceramic fabric weave pattern, to more accurately estimate the radiation heat transfer from the fabric composite surface. Some work has been done on the modelling of the effect of fiber orientation on thermal radiation in fibrous media, where, the fabric was used for the purpose of thermal insulation instead of thermal radiation [25 & 26].

BIBLIOGRAPHY

1. Z. I. Antoniak, B. Webb, J. M. Bates and M. F. Cooper, "Construction and testing of Ceramic Fabric Heat Pipe with Water Working fluid" , Eighth Symposium on Space Nuclear Power Systems, Albuquerque, NM, January, 1991.
2. W. C. Kiestler, T. S. Marks and A. C. Klein "Design and Testing of Fabric Composite Heat Pipes for Space Nuclear Power Systems", in Proc. American Nuclear Society Topical Meeting on Nuclear Technologies for Space Exploration, Jackson Hole, WY, August, 1992.
3. William C. Kiestler, "Heat Pipes Technology Development ", M.S. Thesis, Oregon State University, Corvallis, OR, December, 1992.
4. H. Al-Baroudi and A. C. Klein, "Experimental Simulation of the Bubble Membrane Radiator using a Rotating Flat Plate" , Eighth Symposium on Space Nuclear Power Systems, Albuquerque, NM, January, 1991.
5. M. S. El-Genk and H. Xue, "An Investigation of Natural Circulation Decay Heat Removal From an SP-100 Reactor System For a Lunar Outpost", in Proc. Ninth Symposium on Space Power Systems, Albuquerque, NM, Jan., 1992.
6. R. Siegel and J. Howell, "Thermal Radiation Heat Transfer", 2nd ed., pp 236-248, Hemisphere Publishing Corp., NY, WA, PH, London (UK), 1981.
7. G.G. Gubereff, J. E. Janssen, R. H. Torberg, "Thermal Radiation Properties Survey", 2nd ed., Honeywell Research Center, Minneapolis.
8. Z. I. Antoniak et al, "Fabric Space Radiators", PNL-6458, 1988.
9. Z. I. Antoniak and B. J. Webb, "Fabric Space Radiators" , in Proc. Sixth Symposium on Space Nuclear Power Systems, Albuquerque, NM, 1989.

10. Paul M. Sawko and H.K. Tran' "Strength and Flexibility Properties of Advance Ceramic Fabrics(ACF)", SAMPE Quarterly 17(1):7-13.
11. Z. I. Antoniak, J. M. Bates, B. J. Webb, "Construction & Testing of Advanced Ceramic Fabric Components to 1000 K", in proc. Seventh Symposium on Space Nuclear Power Systems, Albuquerque, NM, January, 1990.
12. T. S. Marks and A. C. Klein, "Materials Compatibility Issues For Fabric Composite Radiators", in Proc. Eighth Symposium on Space Nuclear Power Systems, Albuquerque, NM, January, 1991.
13. T. S. Marks and A. C. Klein "An Experimental Comparison of Wicking Abilities of Fabric Materials for Heat Pipe Applications", in Proc. Ninth Symposium on Space Nuclear Power Systems, Albuquerque, NM, January, 1992.
14. T. S. Marks, "An Investigation of Fabric Composite Heat Pipe Feasibility Issues", M.S. Thesis, Oregon State University, Corvallis, OR, 1992.
15. A. C. Klein, Z. Gulshan Ara, W. C. Kiestler, R. Snuggerud, T. S. Marks, "Fabric Composite Heat Pipe Technology Development", in Proc. Tenth Symposium on Space Nuclear Power Systems, Albuquerque, NM, Jan., 1993.
16. Z. Gulshan Ara and A. C. Klein, "Fabric Composite Heat Transfer Study", in Proc. American Nuclear Society Topical Meeting on Nuclear Technologies for Space Exploration, Jackson Hole, WY, August, 1992.
17. W. A. Ranken, "Heat Pipe Development for the SPAR Space Power System", IVth International Heat Pipe Conference, London, UK, September, 1981.
18. V. C. Truscello and L. L. Rutger, "The SP-100 Power System", in Proc. Ninth Symposium on Space Nuclear Power Systems, AIP-CONF 920104, Albuquerque, NM, January, 1992.

19. M. G. Jacox and A. C. Zuppero, "The SEHPTR Stage: A Thermionic Combined Power and Propulsion Technology for Space Application", in Proc. Nuclear Technologies for Space Exploration 1992, Jackson Hole, WY, 1992.
20. M. A. Merrigan and V. L. Trujillo, "Moderated Heat Pipe Thermionic Reactor (MOHTR) Module Development and Test", in Proc. 9th Symposium on Space Nuclear Power Systems, AIP CONF-920104, Albuquerque, NM, January, 1992.
21. D. Trent, "Numerical Methods for Engineering Analysis", Course Handout, ME573, Oregon State University, Corvallis, OR, 1989.
22. ASME Boiler and Pressure Vessel Code, vol 109, 1986.
23. Bird, Stewart and Lightfoot, "Transport Phenomena", pp 251-252 & 744-745.
24. Homam M. Al-Baroudi, "Experimental Simulations of a Rotating Bubble Membrane Radiator for Space Nuclear Power Systems", Ph D. Thesis, Oregon State University, Corvallis, OR, 1993.
25. S. C. Lee, "Radiative Transfer Through a Fibrous Medium: Allowance for fiber Orientation", in Journal, Quant. Spectrosc., Radiative Transfer, Vol 36, No. 3, 1986.
26. S. C. Lee, "Effect of Fiber Orientation on Thermal Radiation in Fibrous Media", in Int. J. Heat Mass Transfer, 1988.

APPENDICES

APPENDIX AComputer Program Hardcopies:

1. Program for calculating combined conduction-radiation heat transfer through the fabric composite material
2. Program for calculating the configuration factors
3. Program for calculating the effective emissivity

Appendix A1.

```

PROGRAM FCRHT
C*****
C
C          FABRIC COMPOSITE HEAT TRANSFER STUDY
C
C    This Program is Developed to Calculate the Heat Transfer From
C    a Hot Surface Through a Metallic Liner Sheet and a Fabric
C    Covering and then Radiated to a Cold Surface Crossing a Vacuum
C    Using Numerical Method.
C    The Program Uses jacobian Method and Control Volume Approach.
C
C*****
C**  PARAMETER.FOR and PARA.FOR contain all the parameters
C    and COMMON variables
C    -----
C    INCLUDE 'PARAMETER.FOR'
C    COMMON FC
C    COMMON EFFEM,SIGMA

C**  OPEN A LOGICAL UNITS FOR OUTPUT
C    OPEN(UNIT=L1,FILE='FCF.OUT')
C    OPEN(UNIT=L2,FILE='FORPLOT')
C    WRITE(*,100)
C    WRITE(L1,100)
C    WRITE(L2,200)
C    CALL PRESET
C    CALL INPUT
C    CALL SETUP
C    IF(CONTROL(1)) CALL SSTATE
C    IF(.NOT.CONTROL(1)) THEN
C    PRINT*, ' This program does not handle transient cases'
C    ENDIF
C    STOP
100  FORMAT(///10X,
1    ' FABRIC COMPOSITE RADIATION HEAT TRANSFER STUDY'//)
200  FORMAT(6X,'Mesh',7x,'Temperature (K)'/
1    6X,'-----',6x,'-----'//)
C    END
C*****
C    SUBROUTINE PRESET
C    INCLUDE 'PARAMETER.FOR'
C    COMMON FC
C    COMMON EFFEM,SIGMA
C**  PRESET ARRAYS ( DEFINES A COMPLETE SET)
C    DO 10 J = 1,MAX2
C    DO 10 I = 1,MAX1
C        T(I,J) = 0.
C        BETA(I,J) = 0.
C        CX1(I,J) = SMALL
C        CX2(I,J) = SMALL

```

```

      DX1(I,J) = 0.
      DX2(I,J) = 0.
      AR1(I,J) = SMALL          ! SMALL = 1.E-25
      AR2(I,J) = SMALL
      CAY(I,J) = SMALL
      Q(I,J)   = 0.0
      CV(I,J)  = 0.
      MAT(I,J) = 1003
10  CONTINUE
      DT          = 0.
      TYME        = 0.
      DO 20      I = 1,10
          CONTROL(I) = .FALSE.
20  CONTINUE
C-----
C  MATERIAL BOUNDARY CONDITION ID NUMBERS
C  LISTED BELOW ARE THE BOUNDARY MATERIAL ID NUMBERS:
C  ID = 1000 : KAY = 0.0014      - MODEL MATERIAL
C  ID = 1001 : KAY = SMALL      - GRADIENT OF TEMPERATURE
C  ID = 1002 : KAY = BIG        - FIXED TEMPERATURE AT THE
C  BOUNDARY
C  ID = 1003 : KAY = SMALL      - NULL CELL
C  BIG = 1.E+25
C-----
C**  INITIALIZE CONSTANTS
      ITMAX      = 20000
      TCRIT      = 0.001
      TINIT      = 0.
      RETURN
      END
C*****
      SUBROUTINE INPUT
      INCLUDE 'PARAMETER.FOR'
      COMMON FC
      COMMON EFFEM,SIGMA
      CHARACTER * 1 ANS
      CHARACTER * 1 FC
C**  SET DATA
      ANS      = ' '
      WRITE(*,*) ' Steady State Solution ?      (Y OR N) '
      READ (*,1025) ANS
      CONTROL(1) = .FALSE.
      IF(ANS.EQ.'Y'.OR.ANS.EQ.'y') CONTROL(1) = .TRUE.
      PRINT*, ' Using Fabric Composite ?      (y or n) '
      READ(*,1025) FC
      IF(.NOT.CONTROL(1)) GO TO 555
666  CONTINUE
      NMAX1      = 102
      NMAX2      = 3
      IJ         = NMAX1*NMAX2
      DISP(1)    = 2
      DISP(2)    = 2

```

```

DISP(3)      = 5
DISP(4)      = 2
DISP(5)      = 50
DISP(6)      = 2
DISP(13)     = 101
DISP(14)     = 2

C
C**  SET THE BOUNDARY TEMPERATURES (K)
C**  Read Heated Surface Temperature THS First

WRITE(*,*) ' Enter hot surface temperature: '
READ (*,*)  THS

TCS          = 263.          ! Cold surface temperature
TLB          = 300.          ! Side wall temperatures
TRB          = 300.

C
C**  SET THE DX1 AND DX2 ARRAYS (ACTUAL MESH SIZE)
C
DO 110 J = 1,NMAX2
DO 110 I = 1,NMAX1
DX1(I,J) = 0.078
DX2(I,J) = 0.078
110 CONTINUE

C
C**  SET THE AREA ARRAYS: AR1 AND AR2
C
DO 120 J = 2,NMAX2
DO 120 I = 1,NMAX1
AR1(I,J) = DX2(I,J)*1.
AR2(I,J) = DX1(I,J)*1.
120 CONTINUE
NMAXB = NMAX1-51

C
C**  SET THE CELL VOLUMES ( THE ORTHOGONAL JACOBIAN)
C
DO 130 J = 1,NMAX2
DO 130 I = 1,NMAX1
IF(I.EQ.NMAXB) CV(I,J) = AR1(I,J)*1*DX1(I,J)
IF(I.EQ.NMAXB) GO TO 777
CV(I,J) = AR1(I,J)*DX1(I,J)
777 continue
130 CONTINUE

C
C**  SET THE CELL MATERIAL IDENTIFICATION NUMBERS ( FOR THE
C  LIBRARY)
C
IF(FC.EQ.'y') THEN
DO 140 J = 2,NMAX2-1

C**  Loop for Liner material
DO 150 I = 2,51

```

```

      MAT(I,J)    = 1000
150  CONTINUE

C**    Loop for Fabric material
      DO 160 M = 52,60
      MAT(M,J)    = 999
160  CONTINUE

140  CONTINUE

      ELSE
      DO 170 J = 2,NMAX2-1
      DO 180 I = 2,NMAX1-52
      MAT(I,J)    = 1000
180  CONTINUE
170  CONTINUE
      ENDIF

C
C**    SET BOUNDARY CONDITIONS
C
      DO 190 J = 2,NMAX2-1
      MAT(1,J)    = 1002
      T(1,J)      = THS
      TOLD(1,J)   = THS

      MAT(NMAX1,J) = 1002
      T(NMAX1,J)  = TCS
      TOLD(NMAX1,J) = TCS
190  CONTINUE

      DO 195 I = 2,NMAX1-1
      MAT(I,1)    = 1001
      T(I,1)      = TLB
      TOLD(I,1)   = TLB
      MAT(I,NMAX2) = 1001
      T(I,NMAX2)  = TRB
      TOLD(I,NMAX2) = TRB
195  CONTINUE
555  CONTINUE
1025 FORMAT(A1)
      RETURN
      END

C*****
      SUBROUTINE SETUP
      INCLUDE 'PARAMETER.FOR'
C**    ARRAYS FOR OUTPUT FORMATS
      NIX(1)    = 1
      X1(1)     = -.5*DX1(1,1)
      DO 110 I = 2,NMAX1
      X1(I)     = X1(I-1) +.5*(DX1(I-1,1) + DX1(I,1))
      NIX(I)    = I
110  CONTINUE

```

```

      X2(1)      = -.5*DX2(1,1)
      DO 120 J = 2,NMAX2
      X2(J)      = X2(J-1) +.5*(DX2(1,J-1) + DX2(1,J))
120  CONTINUE
      CALL CONNECTOR(1)
      CALL CONNECTOR(2)
      CALL CONNECTOR(3)
      RETURN
      END

```

C*****

```

      SUBROUTINE SSTATE
      INCLUDE 'PARAMETER.FOR'
      common fc
      common effem,sigma
      CHARACTER *1  ANS
      character *1 fc
C**  BEGIN ITERATION LOOPS
C**  THE PROGRAM USES JACOBIAN METHOD
100  CONTINUE
      LSKIP  = 1
      ITERS  = 0
50   CONTINUE
60   CONTINUE
      ANS    = ' '
      WRITE(*,*) ' '
      WRITE(*,*) ' Enter number of lines to skip printing: '
      READ (*,*)  LSKIP
      WRITE(*,*) ' Enter Temperature convergence tolerance: '
      READ (*,*)  TCRIT
      WRITE(*,*) ' Enter initial temperature: current TINIT is
',TINIT
      READ (*,*)  TINIT
      PRINT*, ' Enter Effective Emissivity: '
      READ(*,*)  EFFEM
120  CONTINUE
      WRITE(L1,1003) NMAX1,NMAX2,DX1(1,1),DX2(1,1)ITMAX,
1      TCRIT,TINIT
      WRITE(*,111)
      WRITE(L1,111)
130  CONTINUE
C
C**  SET INITIAL TEMPERATURES IN COMPUTATIONAL REGION
      DO 150 J = 2,NMAX2-1
      DO 150 I = 2,NMAX1-1
          IF(MAT(I,J).LE.1000) T(I,J) = TINIT
          TOLD(I,J)= T(I,J)
150  CONTINUE
200  CONTINUE
C

```


C** Starts the Iteration Loop Here

```

C
    DO 600 M = 1,ITMAX
    ITERS      = ITERS +1
410 CONTINUE
        CALL JACOBI(TUMAX)
500 CONTINUE
    IF(MOD(ITERS,LSKIP).EQ.0) THEN
C** PRINT RESULTS TO HARD COPY DEVICE AND SCREEN
C
    WRITE(*,1005) ITERS,TUMAX,T(DISP(3),DISP(4)),
1      T(DISP(5),DISP(6)),T(DISP(13),DISP(14))
    WRITE(L1,1005) ITERS,TUMAX,T(DISP(3),DISP(4)),
1      T(DISP(5),DISP(6)),T(DISP(13),DISP(14))
    ENDIF
C
C** CHECK CHANGE IN TEMP FOR THIS ITERATION
    IF(TUMAX.LE.TCRIT) THEN
    GO TO 650
    ENDIF
600 CONTINUE
650 CONTINUE
    ANS      = ' '
    WRITE (*,*) ' Enter E to exit or CR to continue with
iteration '
    READ(*,1025) ANS
    IF(ANS.EQ.'E'.OR.ANS.EQ.'e') GO TO 700
    WRITE(*,*) ' NEW TCRIT ?'
    READ (*,*) TCRIT
    GO TO 200
700 CONTINUE
C
C** FIND MAX AND MIN ALONG WITH I,J LOCATIONS
    CALL ASMAX(NMAX1,NMAX2,MAT,T,IMAX,JMAX,TMAX)
    CALL ASMIN(NMAX1,NMAX2,MAT,T,IMIN,JMIN,TMIN)
    WRITE(*,1004) ITERS,TUMAX,TMAX,IMAX,JMAX,TMIN,
1      IMIN,JMIN
    WRITE(L1,1004) ITERS,TUMAX,TMAX,IMAX,JMAX,TMIN,
1      IMIN,JMIN
    IF(FC.EQ.'Y') THEN
    HF = EFFEM*SIGMA*(T(61,2)**4-TCS**4)
    ELSE
    HF = EFFEM*SIGMA*(T(50,2)**4-TCS**4)
    ENDIF
    PRINT*, ' q = ',HF
    WRITE(L1,222) HF
C
C** WRITE OUT TEMPERATURE ARRAY
    CALL AWRITER (1,ITERS,T,'STEADY STATE TEMPERATURE ' )
    ANS      = ' '
    WRITE(*,*) ' Enter q to quit or',
1      ' press space bar to continue with new case '

```

```

      IF(CONTROL(2)) THEN
        WRITE(*,*) '          OR'
      ENDIF
      READ(*,1025) ANS
      IF(ANS.EQ.'Q'.OR.ANS.EQ.'q') STOP
      CONTINUE
      GO TO 100

```

C** OUTPUT FORMATS

```

1001 FORMAT(/30X,'ITERATION DETAILS'/9X,
1'ITER NO.   DELTA-T                               DISPLAY TEMP'/
2   31X,4('T(',I3,',',I3,')',2X)/)
1006 FORMAT(/30X,'ITERATION DETAILS'//2X,
1'ITER NO      DELTA-T   ',4X,'T(3',',',4)',9X,'T(7',',',8)',
2              9X,'T(13',',',14)'/)

1003 FORMAT(/
1/5X,'NUMBER OF CELLS IN X1-DIRECTION, NMAX1 - - - -',I5
2/5X,'NUMBER OF CELLS IN X2-DIRECTION, NMAX2 - - - -',I5
3/5X,'WIDTH  OF CELLS IN X1-DIRECTION, DX1 - - - - -',F10.5
4/5X,'WIDTH  OF CELLS IN X2-DIRECTION, DX2 - - - - -',F10.5
6/5X,'MAXIMUM NUMBER ITERATIONS          , ITMAX - - - -',I5
7/5X,'DELTA-PHI ERROR CRITERION          , TCRIT - - - -',1P,E12.3
9/5X,'INITIAL TEMPERATURE                 , TINIT - - - -',1P,E11.4
B)

1004 FORMAT(/
+25X,'STEADY-STATE SOLUTION SUMMARY '/
1/15X,'Total number of iterations   , ITERS - - - -',I5
2/15X,'Maximum temp change,  LAST   , DTMAX - - - -',F10.5
5/15X,'Maximum system temperature , TMAX - - - -',0P,F10.5
6/15X,'
T(',I3,',',I3,',',I3,',')'
7I3,',')'
8/15X,'Minimum system temperature , TMIN - - - -',F10.5
9/15X,'
T(',I3,',',I3,',',I3,',')'
A I3,',')'
B//)

```

```

1005 FORMAT(2X,I6,F15.5,3F15.5/)
1025 FORMAT(A1)

1030 FORMAT(A10)
111 FORMAT('//')
      ' ,
      1      //1X,'Iteration','      Tumax      ','      T(2,2)  ',
      2      '      T(2,50)  ','      T(2,101)  '/'
222 FORMAT('/'      Heat Flux q = ',F11.4,' Watts/cm**2 '/')
      END
C*****
C
      SUBROUTINE CONNECTOR(MODE)
      INCLUDE 'PARAMETER.FOR'
C**  MODE = 1 CALCULATE THE THERMAL CONDUCTIVITY ARRAY
C**  MODE = 2 CALCULATE THE CONNECTOR ARRAYS
C**  MODE = 3 CALCULATE THE BETA ARRAY
      GO TO (100,200,300),MODE
100  CONTINUE
      CALL PROPLIB
      GO TO 800
200  CONTINUE
C**  COMPUTE CONNECTORS, CX1(I,J) AND CX2(I,J)
      HX1      = BIG
      HX2      = BIG
      DO 250 J = 1,NMAX2-1
      DO 250 I = 1,NMAX1-1
          CX1(I,J) = DX1(I,J)/CAY(I,J)+DX1(I+1,J)/CAY(I+1,J)  +
2./HX1      CX1(I,J) = 2.* AR1(I,J)/CX1(I,J)
          CX2(I,J) = DX2(I,J)/CAY(I,J)+DX2(I,J+1)/CAY(I,J+1)  +
2./HX2      CX2(I,J) = 2.*AR2(I,J)/CX2(I,J)
250  CONTINUE
      GO TO 800
300  CONTINUE
C**  This Array is Needed for Transient Calculations
      DO 350 J = 2,NMAX2-1
      DO 350 I = 2,NMAX1-1
          BETA(I,J) = BETA(I,J)/CV(I,J)
350  CONTINUE
800  CONTINUE
      RETURN
      END
C*****
*****
      SUBROUTINE JACOBI(TEMAX)
      INCLUDE 'PARAMETER.FOR'
      COMMON FC
      COMMON EFFEM,SIGMA
      CHARACTER *1 FC
      SUMQ      = 0.

```

```

TEMAX      = 0.
SIGMA      = 5.729E-12
NMAXB      = NMAX1-51
DO 555 J = 2,NMAX2-1
DO 555 I = 2,NMAX1-1
    Q(I,J) = 0.0
    IF(I.EQ.NMAXB) THEN
        Q(I,J) = Q(I,J)+AR1(I,J)*SIGMA*EFFEM
1          *(TOLD(I,J)**4-TCS**4)
    ENDIF
555 CONTINUE
DO 100 J = 2,NMAX2-1
DO 100 I = 2,NMAX1-1
    IF(MAT(I,J).LE.1000) THEN
        DP      = CX1(I,J)+CX2(I,J)      + CX1(I-1,J)+CX2(I,J-1)
        T(I,J) = (CX1(I,J)*TOLD(I+1,J) + CX1(I-1,J)*TOLD(I-1,J)
+
1          CX2(I,J)*TOLD(I,J+1) + CX2(I,J-1)*TOLD(I,J-1)
+
2          Q(I,J))/DP
        QERR    = T(I,J)
        SUMQ    = SUMQ + ABS(QERR)
        DELT    = T(I,J)-TOLD(I,J)
        TEMAX   = MAX(ABS(DELT),TEMAX)
    ENDIF
100 CONTINUE
    DO 200 J = 2,NMAX2-1
    DO 200 I = 2,NMAX1-1
        TOLD(I,J)= T(I,J)
200 CONTINUE
RETURN
END

```

```

SUBROUTINE PROPLIB
C** LIBRARY INCLUDES MATERIAL PROPERTIES
INCLUDE 'PARAMETER.FOR'
REAL      *8 KAY
CHARACTER*8 RLINER
C** SUBROUTINE COMPUTES SI THERMAL CONDUCTIVITY
C** TC - - DEGREES CENTIGRADE
C** KAY - Watts/cm-Degree C ( OR K)
PRINT*, ' Enter the Symbol of the Liner Material: '
PRINT*, ' Program handles CU, AL, SS, TI: '
READ(*,*) RLINER
DO 700 J = 1,NMAX2
DO 700 I = 1,NMAX1
MATNO = MAT(I,J)

```

500 CONTINUE

C** Metallic Liner Thermal Properties
 C** THS is the Heated Surface Temperature in K

```

IF(MAT(I,J).EQ.1000) THEN
C** copper
  IF(RLINER.EQ.'CU') THEN
    IF(THS.EQ.573.) THEN
      KAY = 3.69
    ELSE IF(THS.EQ.521.) THEN
      KAY = 3.665
    ELSE IF(THS.EQ.376.) THEN
      KAY = 3.59
      RHON = 8.94
      SPHT = 381.0
    END IF
  
```

```

C ** Aluminum
C ** At 573 K
  ELSE IF(RLINER.EQ.'AL') THEN
    IF(THS.EQ.573.) THEN
      KAY = 2.28
  
```

```

C ** At 521 K
  ELSE IF(THS.EQ.521.) THEN
    KAY = 2.20
  
```

```

C ** At 376 K (W/cm)
  ELSE IF(THS.EQ.376) THEN
    KAY = 2.06
    RHON = 2.699
    SPHT = .871
  END IF
  
```

```

C ** Titanium
  ELSE IF(RLINER.EQ.'TI') THEN
    IF(THS.EQ.573.) THEN
      KAY = 2.
    ELSE IF(THS.EQ.521.) THEN
      KAY = 3.
    ELSE IF(THS.EQ.376.) THEN
      KAY = 4.56
      RHON = 1.
      SPHT = 1.
    END IF
  
```

```

C ** Stainless steel
  ELSE IF(RLINER.EQ.'SS') THEN
    IF(THS.EQ.573.) THEN
      KAY = .19
    ELSE IF(THS.EQ.521.) THEN
      KAY = .18
    ELSE IF(THS.EQ.376.) THEN
  
```

```

        KAY = .16
        RHON = 1.
        SPHT = 1.
    END IF
END IF
print*, rliner,kay
END IF

IF(MAT(I,J).EQ.1001) THEN
    KAY = 1.E-30
    RHON = 1.
    SPHT = 1.
ELSE IF(MAT(I,J).EQ.999) THEN
    KAY = 1.3817
    RHON = 2200.0
    SPHT = 963.01
ELSE IF(MAT(I,J).EQ.888) THEN
    KAY = SMALL
    RHON = 1.
    SPHT = 1.
ELSE IF(MAT(I,J).EQ.1002) THEN
    KAY = 1.E+30
    RHON = 1.
    SPHT = 1.
ELSE IF(MAT(I,J).EQ.1003) THEN
    KAY = 1.E-30
    RHON = 1.
    SPHT = 1.
ENDIF
600    CAY(I,J) = KAY
        BETA(I,J) = 1./(RHON*SPHT)
700    CONTINUE
14    format(1x,a8,f8.3)
    RETURN
    END
C*****
*****
SUBROUTINE ASMIN(NMAX1,NMAX2,MAT,A,II,JJ,AMIN)
C**  FIND INDICES LOCATION AND MINIMUM OF A
    INCLUDE 'PARA.FOR'
    REAL *8    A(MAX1,MAX2),AMIN

    DIMENSION  MAT(MAX1,MAX2)

    II        = 2
    JJ        = 2
    AMIN      = A(2,2)
    DO 100 J = 2,NMAX2-1

    DO 100 I = 2,NMAX1-1

        IF(MAT(I,J).LE.1000) THEN

```

```

        IF(A(I,J).LT.AMIN) THEN

            AMIN = A(I,J)

            JJ = J
            II = I
        ENDIF

    ENDIF

100 CONTINUE
    CONTINUE
66  format(5x,'    a(2,2) = ',f15.6)
    RETURN

    END
C*****
    SUBROUTINE ASMAX(NMAX1,NMAX2,MAT,A,II,JJ,AMAX)
C**  FIND INDICES LOCATION AND MAXIMUM OF A

    INCLUDE 'PARA.FOR'
    REAL *8    A(MAX1,MAX2),AMAX

    DIMENSION  MAT(MAX1,MAX2)

CC**  INSERTED ONE LINE
    II = 2
    JJ = 2
    AMAX = A(2,2)
    DO 100 J = 2,NMAX2-1

        DO 100 I = 2,NMAX1-1
            IF(MAT(I,J).LE.1000) THEN

                IF(A(I,J).GT.AMAX) THEN

                    AMAX = A(I,J)

                    JJ = J
                    II = I
                ENDIF

            ENDIF

        DO 100 I = 2,NMAX1-1

    DO 100 J = 2,NMAX2-1

100 CONTINUE
    RETURN

    END

```

```

C*****
      SUBROUTINE AWRITER (MODE,NSTEP,ARRAY,LABEL)
C**   GENERAL REAL ARRAY WRITER
      INCLUDE 'PARAMETER.FOR'
      REAL *8  ARRAY(MAX1,MAX2)
      CHARACTER *32 LABEL

C
C**   TRIM THE TRAILING BLANKS FROM LABEL
C
      DO 10 I = 32,1,-1
      IF(LABEL(I:I).GT.' ') GO TO 20
10    CONTINUE
20    CONTINUE
      IF(MODE.EQ.1) WRITE(L1,1000) LABEL(1:I),NSTEP
      IF(MODE.EQ.2) WRITE(L1,1005) LABEL(1:I),NSTEP,TYME
      N2 = 0
100   CONTINUE
      N1 = N2 + 1
      N2 = N1 + 4
      IF(N2.GT.NMAX1) N2 = NMAX1
      WRITE(L1,1001) (NIX(I),I=N1,N2)
      WRITE(L1,1002) (X1(I),I=N1,N2)
      WRITE(L1,1003) (ARRAY(I,2),I=N1,N2)
      DO 22 I = N1,N2
22    WRITE(L2,21) NIX(I),ARRAY(I,2)

1006  FORMAT(1P,10E11.3)
      IF(N2.NE.NMAX1) GO TO 100
      RETURN
1000   FORMAT(//4X,A32,/,12X,'DISTRIBUTION    FOR    ITERATION
NUMBER:',I5/
1      12X,39('-',))
1001   FORMAT(//1X,'Mesh          = ',5(I8,3X))

1002   FORMAT( 1X,'dist. (cm) = ',5(F10.4,1X))

1003   FORMAT(' Temp.   (K) = ',5F11.5)
1005   FORMAT(//10X,A32,' ARRAY OUTPUT FOR TIME STEP NUMBER:',I5,
1      '    TIME = ',F15.4, ' SECONDS'//)
21    FORMAT(5X,I4,7X,F11.5)
      END

```


C*****

C Parameters for program FCRHT

IMPLICIT REAL *8 (A-H,O-Z)

LOGICAL *4 CONTROL

CHARACTER *1 NEGU, NEGL

PARAMETER (MAX1 =102)

PARAMETER (MAX2 = 03)

PARAMETER (MAXLINE =102)

PARAMETER (NMAT = 15)

PARAMETER (BIG = 1.E+25)

PARAMETER (SMALL = 1.E-25)

PARAMETER (LARGE = 1000000)

PARAMETER (NEGU = 'N')

PARAMETER (NEGL = 'n')

PARAMETER (L1 = 11)

PARAMETER (L2 = 12)

PARAMETER (INP = 21)

COMMON/AS1ZE/ T (MAX1, MAX2), BETA (MAX1, MAX2),

1 CX1 (MAX1, MAX2), CX2 (MAX1, MAX2), ETA (MAX1, MAX2),

2 HC1 (1, 1), HC2 (1, 1), DPHI (MAX1, MAX2), THETA (MAX1, MAX2),

3 DX1 (MAX1, MAX2), DX2 (MAX1, MAX2), R (MAX2),

4 AR1 (MAX1, MAX2), AR2 (MAX1, MAX2), Q (MAX1, MAX2),

5 CAY (MAX1, MAX2), MAT (MAX1, MAX2), CV (MAX1, MAX2),

6 RMAT (NMAT), THETAOLD (MAX1, MAX2), TDIFF (MAX1, MAX2),

7

TOLD (MAX1, MAX2), THDIFF (MAX1, MAX2), THDIFFOLD (MAX1, MAX2),

8 DEL (MAX1, MAX2), PHI (MAX1, MAX2), ALAMDA (MAX1, MAX2)

COMMON/OUTPT/ NIX (MAX1), DISP (30), X1 (MAX1), X2 (MAX2)

COMMON/INTGR/ NMAX1, NMAX2, ITERS, IJ, ITMAX, ITMAXT, LEVEL, NSTEPS

C O M M O N / R E A L S /

OMEGA, QMAX, QERROR, TCRIT, TINIT, PI, THETA1, T1CRIT, PREF

COMMON/REALS/ ALBEHIND, ALENGTH, ALFRONT, HB, HF

COMMON/PARAB/ F, TYME, DT, TSTOP, DTMAX

COMMON/SOLVE/ AP (MAXLINE), AC (MAXLINE), AM (MAXLINE), B (MAXLINE)

COMMON/BCOND/ THS, TCS, TLB, TRB

COMMON/LOGIC/ CONTROL (10)

C PARA.FOR

DIMENSION TSTAR(MAX1,MAX2)
EQUIVALENCE (TSTAR(1,1),ETA(1,1))

C**

IMPLICIT REAL *8 (A-H,O-Z)
LOGICAL *4 CONTROL
CHARACTER *1 NEGU,NEGL

PARAMETER (MAX1 =102)
PARAMETER (MAX2 = 03)
PARAMETER (MAXLINE =102)
PARAMETER (NMAT = 15)
PARAMETER (BIG = 1.E+25)
PARAMETER (SMALL = 1.E-25)
PARAMETER (LARGE = 1000000)
PARAMETER (NEGU = 'N')
PARAMETER (NEGL = 'n')

PARAMETER (L1 = 11)
PARAMETER (L2 = 12)
PARAMETER (INP = 21)

SAVE

***** Sample Output for copper liner *****

FABRIC COMPOSITE RADIATION HEAT TRANSFER STUDY

NUMBER OF CELLS IN X1-DIRECTION, NMAX1 - - - - 102
 NUMBER OF CELLS IN X2-DIRECTION, NMAX2 - - - - 3
 WIDTH OF CELLS IN X1-DIRECTION, DX1 - - - - 0.07800
 WIDTH OF CELLS IN X2-DIRECTION, DX2 - - - - 0.07800
 MAXIMUM NUMBER ITERATIONS , ITMAX - - - -20000
 DELTA-PHI ERROR CRITERION , TCRIT - - - - 1.000E-03
 INITIAL TEMPERATURE , TINIT - - - - 3.0000E+02

*** ITERATION DETAILS ***

Iteration	Tumax	T(2,2)	T(2,50)	T(2,101)
1000	0.05738	369.42651	318.98715	0.00000
2000	0.03553	372.16527	342.09188	0.00000
3000	0.02104	373.73105	355.93128	0.00000
4000	0.01245	374.65721	364.12307	0.00000
5000	0.00737	375.20532	368.97109	0.00000
6000	0.00436	375.52970	371.84020	0.00000
7000	0.00258	375.72167	373.53818	0.00000
8000	0.00153	375.83528	374.54306	0.00000

STEADY-STATE SOLUTION SUMMARY

Total number of iterations , ITERS - - - - 8808
 Maximum temp change, LAST , DTMAX - - - - 0.00100
 Maximum system temperature , TMAX - - - - 375.98455
 Location , T(I,J) - - - T(2, 2)
 Minimum system temperature , TMIN - - - - 375.04640
 Location , T(I,J) - - - T(50, 2)

Heat Flux q = 0.0430 Watts/cm**2

STEADY STATE TEMPERATURE

DISTRIBUTION FOR ITERATION NUMBER: 8808

Mesh	=	1	2	3	4	5
dist. (cm)	=	-0.0390	0.0390	0.1170	0.1950	0.2730
Temp. (K)	=	376.00000	375.98455	375.95371	375.92287	375.89219

Mesh	=	6	7	8	9	10
dist. (cm)	=	0.3510	0.4290	0.5070	0.5850	0.6630
Temp. (K)	=	375.86151	375.83112	375.80073	375.77075	375.74078

Mesh	=	11	12	13	14	15
dist. (cm)	=	0.7410	0.8190	0.8970	0.9750	1.0530
Temp. (K)	=	375.71135	375.68192	375.65316	375.62440	375.59642

Mesh	=	16	17	18	19	20
dist. (cm)	=	1.1310	1.2090	1.2870	1.3650	1.4430
Temp. (K)	=	375.56845	375.54138	375.51431	375.48826	375.46221

Mesh	=	21	22	23	24	25
dist. (cm)	=	1.5210	1.5990	1.6770	1.7550	1.8330
Temp. (K)	=	375.43729	375.41236	375.38867	375.36498	375.34262

Mesh	=	26	27	28	29	30
dist. (cm)	=	1.9110	1.9890	2.0670	2.1450	2.2230
Temp. (K)	=	375.32027	375.29933	375.27840	375.25898	375.23956

Mesh	=	31	32	33	34	35
dist. (cm)	=	2.3010	2.3790	2.4570	2.5350	2.6130
Temp. (K)	=	375.22173	375.20391	375.18775	375.17160	375.15718

Mesh	=	36	37	38	39	40
dist. (cm)	=	2.6910	2.7690	2.8470	2.9250	3.0030
Temp. (K)	=	375.14276	375.13014	375.11752	375.10675	375.09598

Mesh	=	41	42	43	44	45
dist. (cm)	=	3.0810	3.1590	3.2370	3.3150	3.3930
Temp. (K)	=	375.08711	375.07823	375.07129	375.06435	375.05937

Mesh	=	46	47	48	49	50
dist. (cm)	=	3.4710	3.5490	3.6270	3.7050	3.7830
Temp. (K)	=	375.05439	375.05140	375.04840	375.04740	375.04640

Mesh	=	51	52	53	54	55
dist. (cm)	=	3.8610	3.9390	4.0170	4.0950	4.1730
Temp. (K)	=	0.00000	0.00000	0.00000	0.00000	0.00000

Mesh	=	56	57	58	59	60
dist. (cm)	=	4.2510	4.3290	4.4070	4.4850	4.5630
Temp. (K)	=	0.00000	0.00000	0.00000	0.00000	0.00000

Mesh	=	61	62	63	64	65
dist. (cm)	=	4.6410	4.7190	4.7970	4.8750	4.9530
Temp. (K)	=	0.00000	0.00000	0.00000	0.00000	0.00000

Mesh	=	66	67	68	69	70
dist. (cm)	=	5.0310	5.1090	5.1870	5.2650	5.3430
Temp. (K)	=	0.00000	0.00000	0.00000	0.00000	0.00000

Mesh	=	71	72	73	74	75
dist. (cm)	=	5.4210	5.4990	5.5770	5.6550	5.7330
Temp. (K)	=	0.00000	0.00000	0.00000	0.00000	0.00000

Mesh	=	76	77	78	79	80
dist. (cm)	=	5.8110	5.8890	5.9670	6.0450	6.1230
Temp. (K)	=	0.00000	0.00000	0.00000	0.00000	0.00000

Mesh	=	81	82	83	84	85
dist. (cm)	=	6.2010	6.2790	6.3570	6.4350	6.5130
Temp. (K)	=	0.00000	0.00000	0.00000	0.00000	0.00000

Mesh	=	86	87	88	89	90
dist. (cm)	=	6.5910	6.6690	6.7470	6.8250	6.9030
Temp. (K)	=	0.00000	0.00000	0.00000	0.00000	0.00000

Mesh	=	91	92	93	94	95
dist. (cm)	=	6.9810	7.0590	7.1370	7.2150	7.2930
Temp. (K)	=	0.00000	0.00000	0.00000	0.00000	0.00000

Mesh	=	96	97	98	99	100
dist. (cm)	=	7.3710	7.4490	7.5270	7.6050	7.6830
Temp. (K)	=	0.00000	0.00000	0.00000	0.00000	0.00000

Mesh	=	101	102
dist. (cm)	=	7.7610	7.8390
Temp. (K)	=	0.00000	263.00000

Appendix A2.

PROGRAM EMISSIVITY

```

C*****
C
C      This simple FORTRAN program calculates the effective
C      emissivity of the heated fabric composite surface which
C      radiates heat to a cold surface.
C      This program also includes a small error analysis routine to
C      calculate the uncertainty values in the measured parameters.
C
C*****
      PRINT*, ' ENTER VOLT, CURRENT, TH, TL : '
      READ *,   VOLT,CURRENT,TH,TC           ! Temperatures in C
                                              ! Volt in volts
                                              ! Current in amp
                                              ! W/M**2-S-K**4
      SIGMA = 5.729E-08
      TH     = TH+273.0
      TC     = TC+273.0
      POWERO = VOLT*CURRENT                  ! WATTS
      PLOSS  = POWERO/10.
      POWER  = POWERO-PLOSS
      AREA   = (6.0*2.54/100.)*(6.0*2.54/100.) ! M**2

C
C ***** Error Analysis Routine *****
C
      DTH = 2.
      DTC = 2.
      TDIFF = (TH*TH*TH*TH-TC*TC*TC*TC)
      B = AREA*SIGMA*TDIFF
      EPSTH = -(4.*POWER*TH*TH*TH)/TDIFF**2
      EPSTC = (4.*POWER*TC*TC*TC)/TDIFF**2
      EMISS = POWER/B
      DEMISS= SQRT(((EPSTH*DTH)**2)+((EPSTC*DTC)**2))
      PRINT *, ' EMISSIVITY = ',EMISS,'+-',DEMISS
      STOP
      END

```

Appendix A3.

PROGRAM VIEW FACTOR

```

C*****
C
C      This FORTRAN program calculates view factors for different
C      geometries using formula from Reference 6.
C
C*****
      INTEGER OPTION
      REAL l,LC
      PRINT *, 'ENTER OPTION:'
      PRINT *, '
      PRINT *, '1      Identical, Parallel, Directly opposed
                Rectangles'
      PRINT *, '2 Two finite rectangles of same length, with one'
      PRINT *, '      common edge'
      PRINT *, '3 Two concentric cylinders of same finite length'
      PRINT *, '
      READ *, OPTION
      PI = ACOS(-1)
      GO TO (10,20,30) OPTION
10      PRINT *, ' Identical, Parallel, Directly opposed
                Rectangles'
      PRINT *, ' Enter data '
      READ *, a,b,c,A1,A2
      X = a/c
      Y = b/c
      PI= ACOS(-1)
      F12 = (2/(PI*X*Y))*(ALOG(SQRT(((1+X**2)*(1+Y**2)))/
*      (1+X**2+Y**2)))+X*SQRT(1+Y**2)*ATAN(X/SQRT(1+Y**2))
*      +Y*SQRT(1+X**2)*ATAN(Y/SQRT(1+X**2))
*      -X*ATAN(X)-Y*ATAN(Y))
      F21 = A1/A2 * F12
      PRINT *, F12,F21
      GO TO 999

20      PRINT *, '2 finite rectangles of same length, with 1 common
                edge'
      PRINT *, ' Enter data '
      READ *, h,l,w,A1,A2
      HC = h/l
      WC = w/l
C      A1 = l*w
C      A2 = l*w
      F12= 1/PI*WC*(WC*ATAN(1/WC)+HC*ATAN(1/HC)-SQRT(HC**2+WC**2)
*      *ATAN(1/SQRT(HC**2+WC**2))+.25*ALOG(((1+WC**2)
*      *(1+HC**2))/(1+WC**2+HC**2))*((WC**2*(1+WC**2+HC**2))
*      /((1+WC**2)*(WC**2+HC**2)))*WC**2
*      (HC**2*(1+HC**2+WC**2)/((1+HC**2)*(HC**2+WC**2)))*HC**2))
C

```



```

      F21 = A1/A2*F12
      PRINT *, F12,F21
      GO TO 999
30  PRINT *, ' Two concentric cylinders of same finite length '
      PRINT *, 'r1,r2,l :      '
      READ *, r1,r2,l
      RC = r2/r1
      LC = l/r1
      AC = LC**2+RC**2-1
      BC = LC**2-RC**2+1
      A1 = 2.0*PI*r1*l
      A2 = 2.0*PI*r2*l

C
C
      F21 = 1/RC - (1/PI/RC)*((ACOS(BC/AC))-(1/2/LC)*
*      (SQRT((AC+2)**2-(2*RC)**2)*(ACOS(BC/RC/AC))+
*      BC*(ASIN(1/RC))-PI*AC/2))
      F12 = (A2/A1)*F21

C
      F22 = 1-1/RC+(2/PI/RC)*(ATAN((2*SQRT(RC**2-1))/LC))-
*      (LC/2/PI/RC) * (((SQRT(4*RC**2+LC**2))/LC)*
*      (ASIN((4*(RC**2-1) + (LC**2/RC**2)*
*      (RC**2-2))/(LC**2+4*(RC**2-1)))) -
*      (ASIN((RC**2-2)/RC**2))+(PI/2)*
*      (((SQRT(4*RC**2+LC**2))/LC)-1))

      PRINT *, 'F21 = ',F21,' F22 = ',F22,' F12 = ',F12

      GO TO 999

999  STOP
      END

```

APPENDIX BMiscellaneous Tables:

1. Emissivities of various surfaces
2. Additional information about the advanced ceramic fabrics obtained from the manufacturers' brochures

Miscellaneous Tables

Appendix B1

Table B1. Emissivities of Various Surfaces

Stainless Steel (316)

polished	.24 - .31
----------	-----------

Stainless Steel (310)

smooth	.39
--------	-----

Stainless Steel (301)

polished	.16
----------	-----

Aluminum

highly polished	.04 - .06
-----------------	-----------

polished	.095
----------	------

oxidized	.28 - .31
----------	-----------

Copper

polished	.04 - .05
----------	-----------

oxidized	.78
----------	-----

slightly polished	.15
-------------------	-----

Appendix B2

Table B2. Additional Information about the Advanced Ceramic Fabrics Obtained From The Manufacturers' Brochures.

I. Typical properties of NEXTEL 440 woven ceramic fabrics-

Fiber properties:

Composition - Alumina Boria Silica

Density (non-porous) - .11 lb/in³ (3.05 gm/cc)

Tensile strength - 300×10^3 psi (2070 MPa)

Tensile modulus - 27×10^6 psi (187 GPa)

Melt temp. - 3272°F (1800°C)

Other characteristics - Non-oxidizing, non-hygroscopic, essentially chemically resistant, low thermal conductivity, good abrasion resistance.

II. Typical properties of NICALON

Fiber properties:

Composition - Silicon Carbide

Density - 2.55 g/cm³ (lb/in³)

Tensile strength - 430 Ksi

Tensile modulus - 28 Msi

Specific heat - 1.14 J/g °C

Thermal conductivity - 11.622 W/m-s-°C (10 Kcal/mhr°C,
.0277 cal/cm-s-°C)

Other characteristics - highly resistant to oxidation and to chemical attack.

II. Typical properties of ASTROQUARTZ II

ASTROQUARTZ II ceramic fabric is woven from ASTROQUARTZ II fiber yarns with 9779 resin compatible binder. The 9779 yarn binder is compatible with many epoxy, bismaleimide, polyamide and phenolic resin systems. In addition to a proprietary aminosilane coupling agent, 9779 binder contains film formers and lubricants to facilitate weaving.

- fiber softens at 1300°C but never liquifies.
- volatilization begins near 200°C
- chemically stable
- water insoluble, non-hygroscopic, non-toxic.
- should not be used in environments where strong concentrations of alkalies are present.

ASTROQUARTZ II has filament tensile strength of 850,000 psi. Because of its low coefficient of linear expansion, ASTROQUARTZ II offers great dimensional stability. Fibers are flexible, and function well in applications subject to torsion and flexing. ASTROQUARTZ II is transparent to ultraviolet radiation in the 2000 Å and upwards range. It does not form paramagnetic centers, nor does it capture neutrons in high energy applications. It is an excellent electrical insulator and retains these properties at high temperatures. It can be used at temperatures up to 1050°C. Above this temperature slow devitrification or crystallization occurs with loss of flexible mechanical properties.

Composition - Silicon dioxide

Density - 2.20 g/cm³

Mean specific heat (0 - 500°C) - .23 cal/g °C

(963.01 W/kg °C)

Thermal conductivity at 20 °C - .0033 CGS (1.3817 W/m-K)